

Phenomenology of transverse spin: past, present and future

Mariaelena Boglione¹ and Alexei Prokudin²

¹ Dipartimento di Fisica Teorica, Università di Torino, and INFN, Sezione di Torino, Via P. Giuria 1, I-10125 Torino, Italy

² Division of Science, Penn State Berks, Reading, PA 19610, USA

Received: date / Revised version: date

Abstract. We summarize the most significant aspects in the study of transverse spin phenomena over the last few decades, focusing on Semi-Inclusive Deep Inelastic Scattering processes and hadronic production in e^+e^- annihilations. The phenomenology of transverse momentum dependent distribution and fragmentation functions will be reviewed in an in-depth analysis of the most recent developments and of the future perspectives.

PACS. 13.88.+e Polarization in interactions and scattering – 13.60.-r Inclusive production with identified hadrons – 13.85.Ni Photon and charged-lepton interactions with hadrons

1 Past

The importance of the transverse motion of partons bound inside the nucleon and the corresponding azimuthal effects were first pointed out in the 70's by Feynman, Field and Fox [1,2], who realized that the origin of transverse momentum in Drell-Yan processes could be either due to non zero *intrinsic* momentum of partons confined in the nucleon (non-perturbative effect) or to the recoil of gluons radiated off active quarks (perturbative effect). Their papers are the precursors of the Generalized Parton Model (GPM), which is a straightforward generalization of the parton model by inclusion of the transverse quark motion.

Azimuthal asymmetries in unpolarized reactions, such as Drell-Yan production and Semi-Inclusive Deep Inelastic Scattering (SIDIS), play an important role in testing the perturbative and non-perturbative aspects of strong interactions, as it was recognized in the early work by Georgi and Politzer [3], Mendez [4], and Kane, Pumplin, and Repko [5]. It was Robert Cahn [6,7] who first pointed out that $\cos\phi$ asymmetries in SIDIS can easily be generated by intrinsic quark motion: the associated azimuthal modulation is called the “Cahn effect”.

The related QCD evolution of the cross-sections was studied in the 80's, in the pioneering work by Collins-Soper-Sterman (CSS) [8,9]. It was realized that both non-perturbative and perturbative parts should be combined in order to achieve a reliable theoretical description of the corresponding experimental measurements. Yet, it took several decades to develop the appropriate QCD formalism [10] to describe transverse momentum dependent distribution and fragmentation functions (collectively called TMDs).

Simultaneously, an idea of multi-parton quantum mechanical correlations, or the Efremov-Teryaev-Qiu-Ster-

man matrix elements [11,12,13,14], was born. These correlations are suppressed in the leading term contribution to the unpolarized cross-sections, but can be dominant in spin asymmetries; they are important in the so-called “twist-3” approach to factorization. It was later realized that TMD and twist-3 approaches are intimately related [15].

In the 90's two very important correlations of transverse motion and spin were proposed by Sivers [16,17] and Collins [18]. In order to describe the large (left-right) single spin asymmetries (SSAs) in pion production off hadron-hadron scattering, Sivers suggested that they could originate, at leading twist, from the intrinsic motion of quarks in the colliding hadrons generating an inner asymmetry of unpolarised quarks in a transversely polarized hadron, the so-called Sivers effect. He proposed a new Transverse Momentum Dependent (TMD) distribution function, now commonly called the “Sivers function”, which represents the number density of unpolarized partons inside a transversely polarized nucleon. This mechanism was criticized at first as it seemed to violate time-reversal invariance [18], however Brodsky, Hwang and Schmidt proved by an explicit calculation that initial-state interactions in Drell-Yan processes [19] and final-state interactions in SIDIS [20], arising from gluon exchange between the struck quark and the nucleon remnants, can generate a non-zero Sivers asymmetry. The situation was further clarified by Collins [21] who pointed out that, taking correctly into account the gauge links in the TMD distributions, time-reversal invariance does not imply a vanishing Sivers function, but rather a sign difference between the Sivers distribution measured in SIDIS and the same distribution measured in DY. This sign difference is one of the main goals of the next generation of DY measurements, soon to start at the COMPASS-II experiment at CERN [22], at RHIC (BNL) [23] and at Fermilab [24].

In a different approach, Collins proposed a mechanism based on a spin asymmetry in the fragmentation of transversely polarized quarks into a spinless hadron [18], which involved a transverse-momentum dependent (TMD) fragmentation function, called the “Collins function”, which generates a typical azimuthal correlation, later denoted as the “Collins effect”.

At the same time, and over the following years, the Torino-Cagliari group of Anselmino *et al.* proposed the first, pioneering phenomenological studies of asymmetries in hadron-hadron scattering [25, 26, 27, 28]. In principle many different azimuthal correlations can contribute to the large single spin asymmetries measured in inclusive hadro-production from proton-proton scattering [29, 30]: at first it was believed that the Sivers asymmetry would be largely dominant compared to the Collins effect [31], but later it turned out that this was not necessarily the case. Unfortunately, only one azimuthal angle is observed in the reaction, and this information is not sufficient to allow for the separation of the two effects. The situation might be clarified by a combined data analysis of the Sivers and Collins effects in polarized proton-proton scattering and in SIDIS, under the assumption that factorization holds also for hadronic processes, as proposed in Ref. [32]. A phenomenological overview and the experimental state-of-the-art of polarized proton-proton scattering processes is reviewed in the contribution of E. Aschenauer, U. D’Alesio and F. Murgia to this Special Issue.

The idea of correlations and the corresponding transverse momentum dependent functions (TMDs) describing the nucleon structure came to its full fruition in 1995, when Kotzinian first [33] and later Mulders and Tangerman [34, 35] developed a full theoretical description of Drell-Yan and Semi Inclusive Deep Inelastic Scattering cross sections in terms of TMDs. The three well known collinear distribution functions unfold, at leading order in $1/Q$, into eight independent TMDs: the Sivers function is among them, together with the unpolarized and the helicity distribution functions and two manifestations of the transversity function, h_1 and h_{1T}^\perp (the so called “pretzelosity”), related to the density number of transversely polarized partons inside a transversely polarized nucleon. In addition, we find the Boer-Mulders function, h_1^\perp , related to the density number of transversely polarized partons inside an unpolarized nucleon, and two “mixed” functions (later denominated “warm gear” functions) describing the distribution of transversely polarized partons inside longitudinally polarized nucleons, and vice-versa. The picture is simpler for the fragmentation TMDs where, considering only spinless hadrons, only two functions appear: the unpolarized and the Collins TMD FFs.

The phenomenological extraction of the Sivers and Boer-Mulders distribution functions, of transversity and the Collins function and of pretzelosity will be addressed in Sect. 2, together with a brief overview on the most recent extractions of unpolarized TMD PDFs and FFs.

It was only at the beginning of the 21st century, when the new-generation dedicated SIDIS measurements were performed by the HERMES [36] and COMPASS [37] Col-

laborations, that the framework of TMDs could reliably be experimentally tested for the first time. In particular, the first data collected by the HERMES Collaboration using a transversely polarized proton target, showed clear evidence of a non zero transverse SSAs. One of the main advantages of SIDIS is that the Collins and Sivers effects, as well as the other TMD effects, can easily be separated by appropriately weighting the SIDIS cross section: this generates different azimuthal asymmetries, which can be studied one by one. Contrary to what happens in hadro-production, where all TMD effects occur and mix together in the same observable, in SIDIS each of them can be separated and extracted analyzing the same experimental cross section.

Much progress was achieved in the understanding of the 3D nucleon structure by successive data takings, followed by more and more refined analyses of SIDIS measurements [38, 39]. The front end of 3D studies is presently being reached with the new multidimensional analyses and phenomenological studies of SIDIS multiplicities [40, 41, 42, 43], azimuthal modulations [44, 39, 45] and new, pioneering multidimensional measurements of the Sivers and Collins single spin asymmetries [46].

Correlations between the spin of partons and the hadronic transverse momentum, can also be detected by measuring the azimuthal asymmetries generated in e^+e^- annihilations, when two final hadrons are produced in two (almost) opposite jets. In the process $e^+e^- \rightarrow \bar{q}q$ the transverse polarizations of the $\bar{q}q$ pair are correlated, thus the Collins effect is expected to cause correlated azimuthal modulations of the hadrons into which the q and the \bar{q} fragment. In 2006 the Belle Collaboration provided high-precision measurements [47] of such modulations which allowed, shortly after, the first combined extraction of the Collins function and of the transversity distribution [48, 49], which was refined over the years with the successive re-analyses of the Belle data [50, 51] and with the addition of higher statistics measurements of the BaBar Collaboration [52], in the works of several groups [53, 54, 55, 56]. A similar procedure for the extraction of the transversity distribution, which combines SIDIS and e^+e^- data replacing the Collins functions with di-hadron fragmentation functions, has been adopted in Refs. [57, 58, 59].

From a more formal point of view, TMDs have recently received a renewed burst of interest concerning their Q^2 dependence: the Collins-Soper-Sterman (CCS) resummation scheme, originally devised to describe the Drell-Yan (DY) cross section over its full q_T range, was revisited by Collins in his book [10] and by Rogers and Aybat in Ref. [60], and extended to the fully non-collinear case: evolution equations were then formulated for unpolarized TMD distribution and fragmentation functions. Further studies involving the TMD evolution of the Sivers and Collins functions were performed in the following years by several groups, see for example Refs. [61, 62, 63, 54, 55]. For a complete review of TMD factorization and evolution properties, and an exhaustive list of references, we refer the reader to the contribution of T.C. Rogers in this Special Issue.

2 Present

In this Section we will present some of the most recent phenomenological extractions of TMD distribution and fragmentation functions. As anticipated in Sect. 1, we will focus on the Sivers and the Collins functions, which are at present the most well known from a variety of different experimental measurements, followed by transversity (which at present can only be extracted from SIDIS data, in association with a chirally odd fragmentation function), and the Boer-Mulders and pretzelosity functions. First of all, however, it is important to start with the extraction of the unpolarized TMDs, which one has to rely on for the computation of (the denominator of) any azimuthal spin asymmetry.

2.1 Unpolarized TMD distribution and fragmentation functions

The fundamental role of TMDs is already evident in unpolarized cross sections, simply by looking at the transverse momentum distribution of the final hadron or, at order $1/Q$, at the azimuthal dependence of the hadron around the proton direction, see Fig. 1. In Ref. [64] a first investigation of SIDIS unpolarised cross sections was performed, mainly based on the EMC Collaboration experimental data [65,66], gathered from SIDIS experiments at different energies and different targets. This analysis was updated last year [43], by the inclusion of the newest, multidimensional data on the SIDIS multiplicities measured by the HERMES [40] and COMPASS [41] Collaborations.

Let's consider the unpolarized SIDIS process $l(\ell) + N(P) \rightarrow l'(\ell') + h(P_h) + X(P_X)$, in the γ^*N center-of-mass frame, with the virtual photon moving in the positive z direction, as in Fig. 1. We denote by \mathbf{P}_T the transverse momentum of the produced hadron. The azimuthal angle of this hadron ϕ_h is referred to the lepton scattering plane formed by \mathbf{l} and \mathbf{l}' . The unpolarized differential cross section of SIDIS is then

$$\begin{aligned} \frac{d^5\sigma}{dx_B dy dz_h dP_T^2 d\phi_h} &= \frac{\sigma_0 s y}{2} \left\{ F_{UU} + \right. \\ &+ \frac{2(2-y)\sqrt{1-y}}{(1+(1-y)^2)} F_{UU}^{\cos\phi} \cos\phi_h \\ &+ \left. \frac{2(1-y)}{(1+(1-y)^2)} F_{UU}^{\cos(2\phi_h)} \cos(2\phi_h) \right\}, \end{aligned} \quad (1)$$

where $\sigma_0 = \frac{2\pi\alpha_{em}^2}{Q^2} \frac{1+(1-y)^2}{y}$, and one uses the following standard variables

$$x_B = \frac{Q^2}{2P \cdot q}, \quad y = \frac{P \cdot q}{P \cdot l}, \quad z_h = \frac{P \cdot P_h}{P \cdot q}, \quad (2)$$

where α is the fine structure constant, while $Q^2 = -q^2 = -(l - l')^2$ is the virtuality of the exchanged photon. The structure functions $F_{UU}, F_{UU}^{\cos\phi}, F_{UU}^{\cos 2\phi}$ depend on x_B, z_h, Q^2 , and P_T^2 . F_{UU} is the unpolarized structure function

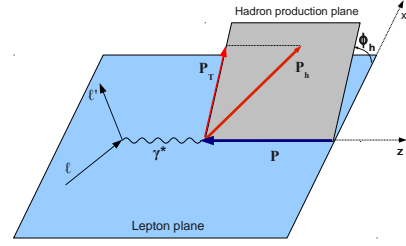


Fig. 1. Kinematical configuration and conventions for SIDIS processes.

which survives upon integration over ϕ_h , over which we are going to concentrate now, while $F_{UU}^{\cos\phi_h}$ and $F_{UU}^{\cos 2\phi_h}$ are associated to the $\cos\phi_h$ and $\cos 2\phi_h$ modulations, respectively, which will be discussed in Sect. 2.4.

If k is the momentum of the quark inside the proton, and \mathbf{k}_\perp its transverse component with respect to the γ^*N axis, in the kinematical region where $P_T \sim k_\perp \ll Q$, the transverse-momentum-dependent (TMD) factorization is known to hold. In this case the structure functions can be expressed in terms of TMD distribution and fragmentation functions, which depend on the light-cone momentum fractions $x \simeq x_B$ and $z \simeq z_h$.

Introducing the transverse momentum \mathbf{p}_\perp of the final hadron with respect to the direction of the fragmenting quark, to order $\mathcal{O}(k_\perp/Q)$, one has

$$\mathbf{P}_T = z\mathbf{k}_\perp + \mathbf{p}_\perp. \quad (3)$$

In the TMD factorization scheme the structure function F_{UU} is given by

$$\begin{aligned} F_{UU} &= x \sum_q e_q^2 \int d^2\mathbf{k}_\perp d^2\mathbf{p}_\perp \delta^{(2)}(z\mathbf{k}_\perp + \mathbf{p}_\perp - \mathbf{P}_T) \times \\ &\times f_{q/p}(x, k_\perp^2) D_{h/q}(z, p_\perp^2) \\ &= x \sum_q e_q^2 \int d^2\mathbf{k}_\perp f_{q/p}(x, k_\perp^2) D_{h/q}(z, (\mathbf{P}_T - z\mathbf{k}_\perp)^2), \end{aligned} \quad (4)$$

where $f_{q/p}(x, k_\perp^2)$ and $D_{h/q}(z, p_\perp^2)$ are the unpolarized TMD distribution and fragmentation function, respectively, for the flavor q (the sum is intended to be both over quarks and antiquarks). At this stage, the Q^2 dependence of all functions is omitted for simplicity.

In most phenomenological models, the $x(z)$ and $k_\perp(p_\perp)$ dependences are factorized and the k_\perp and p_\perp dependences are assumed to be Gaussian, with one free parameter which fixes the Gaussian width,

$$f_{q/p}(x, k_\perp) = f_{q/p}(x) \frac{e^{-k_\perp^2/\langle k_\perp^2 \rangle}}{\pi \langle k_\perp^2 \rangle} \quad (5)$$

$$D_{h/q}(z, p_\perp) = D_{h/q}(z) \frac{e^{-p_\perp^2/\langle p_\perp^2 \rangle}}{\pi \langle p_\perp^2 \rangle}. \quad (6)$$

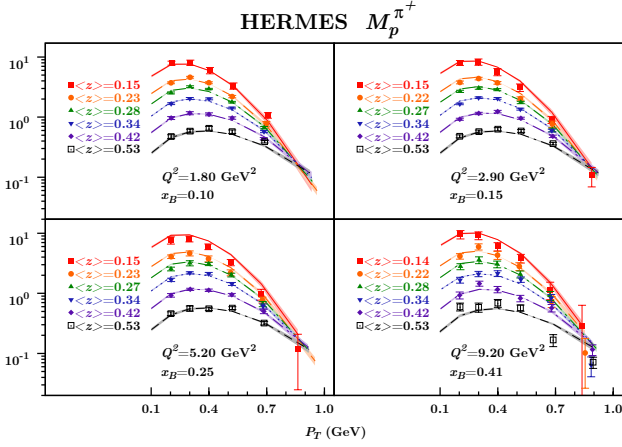


Fig. 2. The multiplicities $M_p^{\pi^+}$ obtained from Eqs. (11) and (8), with the parameters of Eq. (12), are compared with HERMES measurements for π^+ SIDIS production off a proton target [40]. The shaded uncertainty bands correspond to a 5% variation of the total χ^2 . Plot from Ref. [43].

The integrated PDFs, $f_{q/p}(x)$ and $D_{h/q}(z)$, can be taken from the available fits of the world data. In general, the widths of the Gaussians could depend on x or z and might be different for different distributions. Ref. [43] assumes flavour independence and one obtains

$$F_{UU} = x \sum_q e_q^2 f_{q/p}(x_B) D_{h/q}(z_h) \frac{e^{-P_T^2/\langle P_T^2 \rangle}}{\pi \langle P_T^2 \rangle} \quad (7)$$

where

$$\langle P_T^2 \rangle = \langle p_\perp^2 \rangle + z_h^2 \langle k_\perp^2 \rangle. \quad (8)$$

The constant Gaussian parameterization, supported by a number of experimental evidences [67] as well as by dedicated lattice simulations [68], has the advantage that the intrinsic transverse momentum dependence of the cross section can be integrated out analytically. The differential hadron multiplicity (according to the HERMES [40] definition) is

$$M_n^h(x_B, Q^2, z_h, P_T) \equiv \frac{1}{\frac{d^2 \sigma^{DIS}(x_B, Q^2)}{dx_B dQ^2}} \frac{d^4 \sigma(x_B, Q^2, z_h, P_T)}{dx_B dQ^2 dz_h dP_T}. \quad (9)$$

where the index n denotes the kind of target.

The Deep Inelastic Scattering (DIS) cross section has the usual leading order collinear expression,

$$\frac{d^2 \sigma^{DIS}(x_B, Q^2)}{dx_B dQ^2} = y \sigma_0 \sum_q e_q^2 f_{q/p}(x_B). \quad (10)$$

Then, multiplicities are simply given by

$$\begin{aligned} \frac{d^2 n^h(x_B, Q^2, z_h, P_T)}{dz_h dP_T^2} &= \frac{1}{2P_T} M_n^h(x_B, Q^2, z_h, P_T) \\ &= \frac{\pi \sum_q e_q^2 f_{q/p}(x_B) D_{h/q}(z_h) e^{-P_T^2/\langle P_T^2 \rangle}}{\sum_q e_q^2 f_{q/p}(x_B) \pi \langle P_T^2 \rangle}, \end{aligned} \quad (11)$$

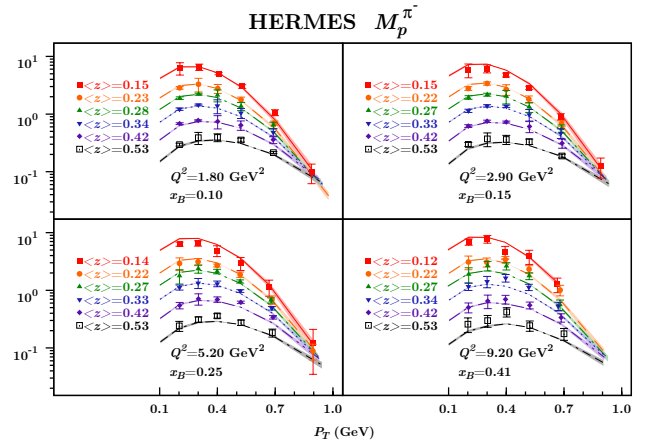


Fig. 3. The multiplicities $M_p^{\pi^-}$ obtained from Eqs. (11) and (8), with the parameters of Eq. (12), are compared with HERMES measurements for π^- SIDIS production off a proton target [40]. The shaded uncertainty bands correspond to a 5% variation of the total χ^2 . Plot from Ref. [43].

with $\langle P_T^2 \rangle$ given in Eq. (8). Notice that, by integrating the above equation over \mathbf{P}_T , with its magnitude ranging from zero to infinity, one recovers the ratio of the usual leading order cross sections in terms of collinear PDFs and FFs. Its agreement with experimental data has been discussed, for instance, in Refs. [40] and [42].

In Fig. 2 we show, as an example, the comparison between the HERMES measurements of the multiplicities for π^+ SIDIS production off a proton target [40] and those obtained in Ref. [43] by best fitting the HERMES multi-dimensional data using the expressions of Eqs. (11) and (8). Notice that this fit, which is performed over a sample of about 500 experimental points, relies on two free parameters only: the two Gaussian widths of the k_\perp and p_\perp distributions of the unpolarized PDF and FF TMDs. The normalization is *not* fixed by adding extra-parameters, as it was done in other analyses like, for instance, Ref. [69]. This simple TMD Gaussian parameterization, with constant and flavour independent widths, delivers a very satisfactory description of the HERMES data points over large ranges of x , z , P_T and Q^2 : the extracted reference values, corresponding to a total χ_{dof}^2 of 1.69, are

$$\begin{aligned} \langle k_\perp^2 \rangle &= 0.57 \pm 0.08 \text{ GeV}^2 \\ \langle p_\perp^2 \rangle &= 0.12 \pm 0.01 \text{ GeV}^2. \end{aligned} \quad (12)$$

These values are obtained by selecting 497 data points corresponding to the following requirements: $Q^2 > 1.69 \text{ GeV}^2$, $0.2 < P_T < 0.9 \text{ GeV}$ and $z < 0.6$. By relaxing the cuts on z in such a way to include one more bin, $z < 0.7$, which increases the number of fitted data points to 576, the quality of the fits deteriorates considerably, giving $\chi_{\text{dof}}^2 = 2.62$, and the extracted Gaussian widths recover values closer to those obtained in previous analyses, like [64] $\langle k_\perp^2 \rangle = 0.46 \pm 0.09 \text{ GeV}^2$ and $\langle p_\perp^2 \rangle = 0.13 \pm 0.01 \text{ GeV}^2$.

HERMES multiplicities do not show any significant sensitivity to additional free parameters: the fits do not

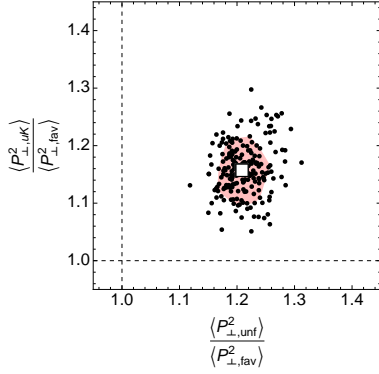


Fig. 4. Distribution of the values of the ratios $\langle P_{\perp, unf}^2 \rangle / \langle P_{\perp, fav}^2 \rangle$ vs. $\langle P_{\perp, uK}^2 \rangle / \langle P_{\perp, fav}^2 \rangle$. The white squared box indicates the center of the 68% confidence interval for each ratio. The shaded area represents the two-dimensional 68% confidence region around the white box. The dashed lines correspond to the ratios being unity; their crossing point corresponds to the result with no flavor dependence. For all points, $P_{\perp, fav}^2 < P_{\perp, unf}^2 \sim P_{\perp, uK}^2$. Plot from Ref. [42].

improve by introducing a z -dependence in the Gaussian widths of the TMD-FFs or by allowing a flavour dependence in the Gaussian widths of the TMD-PDFs. We only find a slight improvement in χ^2 by using different (constant) Gaussian widths in the TMD-FFs; the disfavoured fragmentation functions show a preference for a width slightly wider than that of the favoured fragmentation functions. These results are in agreement with a similar study, performed by Signori et al. in Ref. [42], in which more elaborate input parameterizations were used to model the PDF and FF TMDs ($\langle k_{\perp}^2 \rangle$ ($\langle p_{\perp}^2 \rangle$)) were assigned a particular $x(z)$ and flavour dependence). However, on the basis of a study performed by fitting 200 replicas of the original data points, the authors claim the evidence of a much stronger flavour dependence of the Gaussian p_{\perp} distributions in the fragmentation functions, see Fig. 4.

It is important to observe that in the SIDIS multiplicities, the two free parameters $\langle k_{\perp}^2 \rangle$ and $\langle p_{\perp}^2 \rangle$ are strongly (anti)correlated, as they appear in the combination $\langle P_T^2 \rangle = z_h^2 \langle k_{\perp}^2 \rangle + \langle p_{\perp}^2 \rangle$, see Eq. (7) and (11). Consequently, they can only be uniquely determined by fitting simultaneously two or more different observables. An attempt in this direction has been made by V. Barone et al. in Ref. [45], as we will discuss in Sect. 2.4.

As anticipated above, the COMPASS collaboration has also provided their measurements of SIDIS multiplicities, in multidimensional bins of definite Q^2 and x_B values, each for several values of z_h and P_T , with much higher statistics compared to the HERMES experiment. Fitting COMPASS data, however, turns out to be more difficult: while the Gaussian shape of the P_T dependence is qualitatively well reproduced, there are some unresolved issues with their relative overall normalisation, possibly related to a mistreatment of radiative corrections. The COMPASS fit of Ref. [43], performed by applying an “ad hoc”, y -dependent correction of the bin normalization, returns a

$\langle p_{\perp}^2 \rangle$ TMD-FF Gaussian width slightly larger than that extracted from the HERMES multiplicities, while it delivers similar $\langle k_{\perp}^2 \rangle$ values. Notice that this analysis has been performed on the 2004 run data, when the COMPASS detector was not yet completely set up and no RICH was installed for final hadron separation. Future analyses of more recent COMPASS data with hadron identification and a proper treatment of the radiative corrections should help to clarify the situation.

The study of the Q^2 dependence of SIDIS multiplicities deserves a dedicated discussion.

In the analysis of Ref. [42] no scale dependence was taken into account, while in Ref. [43], with the phenomenological parameterization of Eqs. (5) and (6), the only dependence on Q^2 was included in the collinear part of the TMD, *i.e.* in the collinear PDF or FF factor. The width of the Gaussian, which gives the k_{\perp} (p_{\perp}) dependence of the TMDs, did not include any scale dependence. However Anselmino et al. tried, in Ref. [43] an alternative parameterizations, to allow for a Q^2 and/or x -dependence of the Gaussian widths. As the SIDIS cross section is not sensitive to the individual contributions of $\langle k_{\perp}^2 \rangle$ and $\langle p_{\perp}^2 \rangle$, but only to their linear combination, $\langle P_T^2 \rangle$, see Eqs. (7) and (8), a simplified form can be considered:

$$\langle P_T^2 \rangle = g_1' + z^2 [g_1 + g_2 \ln(Q^2/Q_0^2) + g_3 \ln(10 e x)]. \quad (13)$$

For the HERMES data they did not find any significant x or Q^2 dependence in the transverse momentum spectra, confirming the good agreement of the measured multiplicities with the most simple version of the Gaussian model. For the COMPASS data, instead, some improvement in the quality of the fit can actually be obtained. However, due to the unresolved normalization issues discussed above, it is difficult to give any clear interpretation of this sensitivity and to draw, at this stage, any definite conclusion.

Indeed, it is quite possible that the span in Q^2 of the available SIDIS data is not yet large enough to perform a safe analysis of TMD evolution based only on these data. Another important issue is that, always considering the SIDIS data set, the values of P_T , while being safely low, are sometimes close to Q and corrections to the TMD factorisation scheme might be still relevant.

As a matter of fact, in order to describe the SIDIS cross section over a wide region of P_T (or, more appropriately, of $q_T = P_T/z$) soft gluon resummation has to be performed. This can be done, in the impact parameter b_T space, using for instance the Collins-Soper-Sterman (CSS) formalism or the improved TMD framework of ref. [10]. However, its successful implementation is affected by a number of practical difficulties: the strong influence of the kinematical details of the SIDIS process, the possible dependence on the parameters used to model the non-perturbative content of the SIDIS cross section, the complications introduced by having to perform phenomenological studies in the b_T space, where the direct connection to the conjugate q_T space is lost. Then, a matching prescription has to be applied to achieve a reliable description of the SIDIS process over the full q_T range, going smoothly from the region of

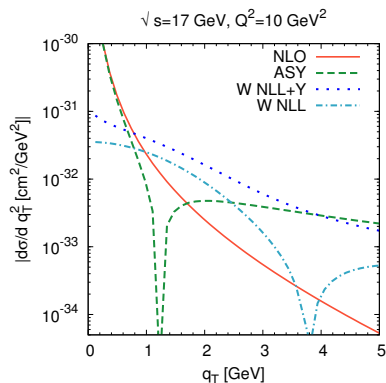


Fig. 5. $d\sigma^{NLO}$, $d\sigma^{ASY}$, W^{NLL} and the sum $W^{NLL} + Y$ corresponding to the SIDIS kinematical configuration of the COMPASS experiment. Plot from Ref. [70].

applicability of resummation, or equivalently of the TMD description, to the region of applicability of perturbative QCD.

A very thorough study of the issues related to matching the perturbative and non-perturbative contributions in SIDIS processes was performed in Ref. [70]. To take care of the non-perturbative content, in Ref. [70] the so-called b_* prescription was adopted in order to cure the problem of the Landau pole in the perturbative expansion, complementing it with the introduction of a properly defined non-perturbative function. Studying the dependence of the cross section on this non-perturbative contribution and on the details of the b_* prescription, i.e. on b_{max} , it was found that some kinematical configurations, similar to those of COMPASS or HERMES experiments for example, are completely dominated by these features. As a consequence, no matching can be achieved exploiting the usual “Y-term prescription”, based on a smooth switch from the $d\sigma^{NLO}$ cross section, calculated perturbatively to NLO, to the next to leading logarithm (NLL) resummed cross section W^{NLL} through the so called Y-term, defined as $Y = d\sigma^{NLO} - d\sigma^{ASY}$, see Fig. 5. Notice that, at large q_T , $d\sigma^{ASY}$ becomes negative and therefore unphysical (we show the absolute value of the asymptotic NLO cross section in Fig. 5 as a dashed, green line). Consequently, the Y term can become much larger than the NLO cross section in that region. This is because the Y term, being calculated in perturbative QCD, does not include any non-perturbative content.

As the mismatch between W^{NLL} and $d\sigma^{ASY}$ at $q_T \sim Q$ is mainly due to the non-perturbative content of the cross section, which turns out to be non-negligible, one could experiment different and more elaborate matching prescriptions, which take into account the non-perturbative contributions to the total cross section. One could require, for instance, that in a region of sizable q_T

$$d\sigma^{total} = W^{NLL} - W^{FXO} + d\sigma^{NLO}, \quad (14)$$

where W^{FXO} is the NLL resummed cross section approximated at first order in α_s , with a first order expansion

of the Sudakov exponential. However, as it was shown in Ref. [70], this method still presents several difficulties and remains largely unsatisfactory. In order to find the origin of these difficulties, Boglione et al. [70] studied in detail the b_T behavior of the perturbative Sudakov factor and found that in a COMPASS-like kinematical configuration the perturbative Sudakov exponential is larger than one, i.e. unphysical, over most of the b_T range. Therefore any resummation scheme would be inadequate in this case, and hardly applicable.

Indeed, being the non-perturbative details of such importance to the description of the cross sections, a critical re-examination of the definition and implementation of the Y-term is needed.

We conclude that, at this stage, it is of crucial importance to have experimental data available in order to test all the mechanisms developed in the resummation of soft gluon emissions and study the non-perturbative aspects of the nucleon. It is essential to have (and analyze) data from HERA ($\sqrt{s} = 300$ GeV), Electron-Ion Collider ($\sqrt{s} = 20 - 100$ GeV), COMPASS ($\sqrt{s} = 17$ GeV), HERMES ($\sqrt{s} = 7$ GeV), and Jefferson Lab 12 ($\sqrt{s} = 5$ GeV). In particular, it will be very important to study experimental data on q_T distributions that span from the region of low $q_T \ll Q$ up to the region of $q_T \sim Q$.

2.2 Sivers Function

Among all TMDs the Sivers function, which describes the number density of unpolarized quarks inside a transversely polarized proton, has so far received the widest attention, from both phenomenological and experimental points of view.

The Sivers function f_{1T}^\perp is related to initial and final state interactions and could not exist without the contribution of the orbital angular momentum of partons to the spin of the nucleon, to which it can be related, in a model dependent way, through the so-called “lensing function” [71]. As such it encodes the correlation between the partonic intrinsic motion and the transverse spin of the nucleon, and it generates a dipole deformation in momentum space: Fig. 6, taken from the EIC White Paper [72], shows the density distribution of unpolarized up and down quarks in a transversely polarized nucleon. For an overview of studies on the parton orbital angular momentum we refer the reader to the contribution of Liu and Lorcé in this Topical Issue.

Over the years, the Sivers function has been extracted from SIDIS data by several groups, with consistent results [73, 74, 75, 76, 77, 78]. However, until very recently, all phenomenological fits had been performed by using a simplified version of the TMD factorization scheme, in which the QCD scale dependence of the TMDs – which was unknown – was either neglected or limited to the collinear part of the unpolarized PDFs. While this might not be a serious numerical problem when considering only experimental data which cover limited ranges of low Q^2 values, it is not correct in principle, and taking into account the appropriate Q^2 evolution might be numerically relevant for

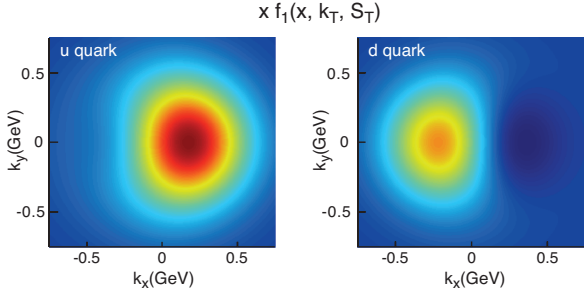


Fig. 6. The 3D density, in the transverse-momentum plane, of unpolarized up and down quarks inside a transversely polarized proton, described by the Siverson function. Here the model of [73] is used and the longitudinal momentum fraction is fixed to $x = 0.1$. The color code indicates the probability of finding the up or down quarks: the deep red (blue) indicates large negative (positive) values for the Siverson function. Plot from Ref. [72]

predictions at higher Q^2 values, like future electron-ion or electron-nucleon colliders (EIC/ENC) and Drell-Yan experiments.

Recently the issue of the QCD evolution of unpolarized TMDs and of the Siverson function has been studied in a series of papers [10,60,61,79,80] where a TMD factorization framework has been worked out for the treatment of SIDIS data and the extraction of polarized TMDs. The main difficulty, here, is due to the fact that the TMD formalism originally developed to describe the Q^2 evolution of the unpolarized TMDs cannot be directly applied to the spin dependent distribution functions, like the Siverson function [16], for which the collinear limit corresponds to twist-3 Qiu-Sterman function T_F . Compared to the unpolarized TMD evolution scheme, the extra aid of a phenomenological input function is required: this input function embeds the missing information on the evolved function, that, in the case of the Siverson function, is both of perturbative and non-perturbative nature.

The TMD Siverson distribution can be extracted by fitting the HERMES and COMPASS SIDIS data on the azimuthal moment $A_{UT}^{\sin(\phi_h - \phi_S)}$. The relevant part of the SIDIS cross-section for Siverson asymmetry reads:

$$\frac{d^5\sigma(S_\perp)}{dx_B dy dz_h d^2P_T} = \sigma_0(x_B, y, Q^2) \left[F_{UU} + \sin(\phi_h - \phi_S) F_{UT}^{\sin(\phi_h - \phi_S)} + \dots \right], \quad (15)$$

where S_T is transverse polarization, and ϕ_h, ϕ_S are the azimuthal angles of the produced hadron and the polarization vector. The spin structure function $F_{UT}^{\sin(\phi_h - \phi_S)}$ is a convolution of the Siverson function f_{1T}^\perp with the unpolarized FF $D_{h/q}$. The ellipsis in Eq. (15) denotes contributions from other spin structure functions.

The experimentally measured Siverson asymmetry is then

$$A_{UT}^{\sin(\phi_h - \phi_S)} \equiv \langle 2 \sin(\phi_h - \phi_S) \rangle \sim \frac{f_{1T}^\perp \otimes D_{h/q}}{f_{q/p} \otimes D_{h/q}} \quad (16)$$

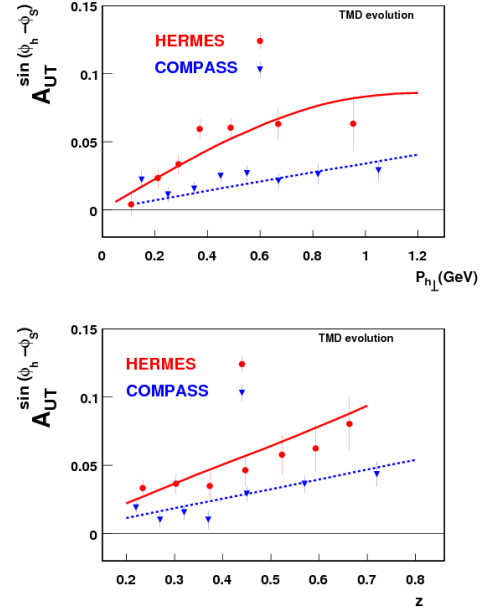


Fig. 7. Comparison between HERMES [82] and preliminary COMPASS data [83] for the z and P_T dependence of the Siverson asymmetry. The solid line is the fit from Ref. [81]. The dashed curve is the result of evolving to the COMPASS scale using the TMD-evolution scheme of Ref. [61]. Plot from Ref. [62].

A first application of the new TMD evolution equations of Ref. [61] to some limited samples of the HERMES and COMPASS data [62] was proposed by Aybat et al. in Ref. [62]. There, it was explicitly shown that the evolution of an existing fit of the Siverson SIDIS asymmetry [81] from the average value $\langle Q^2 \rangle = 2.4 \text{ GeV}^2$ (HERMES [82]) to the average value of $\langle Q^2 \rangle = 3.8 \text{ GeV}^2$ (COMPASS [83]), proved to be reasonably compatible with the TMD evolution equations of Ref. [61]. Their results are shown in Fig. 7.

Shortly afterwards Anselmino, Boglione and Melis [63] performed a complete best fit of the SIDIS Siverson asymmetries taking into account the different Q^2 values of each data point and the Q^2 dependence of the TMDs and compared their results with a similar analysis performed without the TMD evolution. By following Ref. [61], and denoting by \tilde{F} either the unpolarized parton distribution, the unpolarized fragmentation function, or the first derivative, with respect to the parton impact parameter b_T , of the Siverson function, the QCD evolution of the TMDs in the coordinate space can be written as

$$\tilde{F}(x, b_T; Q) = \tilde{F}(x, b_T; Q_0) \times \tilde{R}(Q, Q_0, b_T) \exp \left\{ -g_K(b_T) \ln \frac{Q}{Q_0} \right\}, \quad (17)$$

with

$$\tilde{R}(Q, Q_0, b_T) \equiv \exp \left\{ \ln \frac{Q}{Q_0} \int_{Q_0}^{\mu_b} \frac{d\mu'}{\mu'} \gamma_K(\mu') + \dots \right\}$$

$$\int_{Q_0}^Q \frac{d\mu}{\mu} \gamma_F \left(\mu, \frac{Q^2}{\mu^2} \right) \} \quad (18)$$

and the anomalous dimensions γ_F and γ_K given by

$$\begin{aligned} \gamma_F(\mu; \frac{Q^2}{\mu^2}) &= \alpha_s(\mu) \frac{C_F}{\pi} \left(\frac{3}{2} - \ln \frac{Q^2}{\mu^2} \right) \\ \gamma_K(\mu) &= \alpha_s(\mu) \frac{2C_F}{\pi} . \end{aligned} \quad (19)$$

The Q^2 evolution is driven by the functions $g_K(b_T)$ and $\tilde{R}(Q, Q_0, b_T)$. While the latter, Eq. (18), can be easily evaluated, numerically or even analytically, the former, is essentially unknown and will need to be taken from independent experimental inputs.

The explicit expression of the TMDs in the momentum space, with the QCD Q^2 dependence, can be obtained by Fourier-transforming Eq. (17), obtaining [61]:

$$\hat{f}_{q/p}(x, k_\perp; Q) = \frac{1}{2\pi} \int_0^\infty db_T b_T J_0(k_\perp b_T) \tilde{f}_{q/p}(x, b_T; Q) \quad (20)$$

$$\hat{D}_{h/q}(z, p_\perp; Q) = \frac{1}{2\pi} \int_0^\infty db_T b_T J_0(k_T b_T) \tilde{D}_{h/q}(z, b_T; Q) \quad (21)$$

$$\hat{f}_{1T}^{\perp f}(x, k_\perp; Q) = \frac{-1}{2\pi k_\perp} \int_0^\infty db_T b_T J_1(k_\perp b_T) \tilde{f}_{1T}^{\perp q}(x, b_T; Q), \quad (22)$$

where J_0 and J_1 are Bessel functions. $\hat{f}_{1T}^{\perp q}$ is the Siverts distribution defined, for unpolarized partons inside a transversely polarized proton, as:

$$\begin{aligned} \hat{f}_{q/p^\uparrow}(x, \mathbf{k}_\perp, \mathbf{S}; Q) &= \\ &= \hat{f}_{q/p}(x, k_\perp; Q) - \hat{f}_{1T}^{\perp q}(x, k_\perp; Q) \frac{\epsilon_{ij} k_\perp^i S^j}{M_p} = \end{aligned} \quad (23)$$

$$= \hat{f}_{q/p}(x, k_\perp; Q) + \frac{1}{2} \Delta^N \hat{f}_{q/p^\uparrow}(x, k_\perp; Q) \frac{\epsilon_{ij} k_\perp^i S^j}{k_\perp}. \quad (24)$$

The unknown functions inside Eq. (17), $g_K(b_T)$ and $\tilde{F}(x, b_T; Q_0)$, are then parameterized as

$$g_K(b_T) = \frac{1}{2} g_2 b_T^2 \quad (25)$$

$$\tilde{f}_{q/p}(x, b_T; Q_0) = f_{q/p}(x, Q_0) \exp \{ -\alpha^2 b_T^2 \} , \quad (26)$$

where g_2 is a parameter which should be extracted from experimental data, while the value of α^2 is fixed by requiring the desired behavior of the distribution function in the transverse momentum space at the initial scale Q_0 : taking $\alpha^2 = \langle k_\perp^2 \rangle / 4$ one recovers

$$\hat{f}_{q/p}(x, k_\perp; Q_0) = f_{q/p}(x, Q_0) \frac{1}{\pi \langle k_\perp^2 \rangle} e^{-k_\perp^2 / \langle k_\perp^2 \rangle} , \quad (27)$$

in agreement with Eq. (5).

Similar relations hold for the TMD FFs, with an additional z^2 factor.

Analogously, we parameterize the Siverts function at the initial scale Q_0 as

$$\tilde{f}_{1T}^{\perp}(x, b_T; Q_0) = -2\gamma^2 f_{1T}^{\perp}(x; Q_0) b_T e^{-\gamma^2 b_T^2} , \quad (28)$$

which, when Fourier-transformed according to Eq. (22), yields:

$$\hat{f}_{1T}^{\perp}(x, k_\perp; Q_0) = f_{1T}^{\perp}(x; Q_0) \frac{1}{4\pi\gamma^2} e^{-k_\perp^2 / 4\gamma^2} . \quad (29)$$

Eq. (29) agrees with the usual parameterization of the Siverts function [78, 81, 84], at the initial scale Q_0 , taking:

$$4\gamma^2 \equiv \langle k_\perp^2 \rangle_S = \frac{M_1^2 \langle k_\perp^2 \rangle}{M_1^2 + \langle k_\perp^2 \rangle} \quad (30)$$

$$f_{1T}^{\perp}(x; Q_0) = -\frac{M_p}{2M_1} \sqrt{2e} \Delta^N f_{q/p^\uparrow}(x, Q_0) \frac{\langle k_\perp^2 \rangle_S}{\langle k_\perp^2 \rangle} , \quad (31)$$

where M_1 is a mass parameter, M_p the proton mass and $\Delta^N f_{q/p^\uparrow}(x, Q_0)$ is the x -dependent term of the Siverts function, evaluated at the initial scale Q_0 and written as [78, 81, 84]:

$$\Delta^N f_{q/p^\uparrow}(x, Q_0) = 2\mathcal{N}_q(x) f_{q/p}(x, Q_0) , \quad (32)$$

where $\mathcal{N}_q(x)$ is a function of x , properly parameterized.

The final evolution equations of the unpolarized TMD PDFs and TMD FFs, in the configuration space, are then

$$\begin{aligned} \tilde{f}_{q/p}(x, b_T; Q) &= f_{q/p}(x, Q_0) \tilde{R}(Q, Q_0, b_T) \times \\ &\exp \left\{ -b_T^2 \left(\alpha^2 + \frac{g_2}{2} \ln \frac{Q}{Q_0} \right) \right\} \end{aligned} \quad (33)$$

$$\begin{aligned} \tilde{D}_{h/q}(z, b_T; Q) &= \frac{1}{z^2} D_{h/q}(z, Q_0) \tilde{R}(Q, Q_0, b_T) \times \\ &\exp \left\{ -b_T^2 \left(\beta^2 + \frac{g_2}{2} \ln \frac{Q}{Q_0} \right) \right\} , \end{aligned} \quad (34)$$

with $\alpha^2 = \langle k_\perp^2 \rangle / 4$, $\beta^2 = \langle p_\perp^2 \rangle / (4z^2)$, g_2 given in Eq. (25) and $\tilde{R}(Q, Q_0, b_T)$ in Eq. (18).

The evolution of the Siverts function is obtained through its first derivative, inserting Eq. (28) into Eq. (17):

$$\begin{aligned} \tilde{f}_{1T}^{\perp}(x, b_T; Q) &= -2\gamma^2 f_{1T}^{\perp}(x; Q_0) \tilde{R}(Q, Q_0, b_T) \times \\ &b_T \exp \left\{ -b_T^2 \left(\gamma^2 + \frac{g_2}{2} \ln \frac{Q}{Q_0} \right) \right\} \end{aligned} \quad (35)$$

with γ^2 and $f_{1T}^{\perp}(x; Q_0)$ given in Eqs. (30)-(32).

Eqs. (33)-(35) show that the Q^2 evolution is controlled by the logarithmic Q dependence of the b_T Gaussian width, together with the factor $\tilde{R}(Q, Q_0, b_T)$: for increasing values of Q^2 , they are responsible for the typical broadening effect already observed in Refs. [60] and [61].

It is important to stress that although the structure of Eq. (33) is general and holds over the whole range of b_T values, the input function $\tilde{F}(x, \mathbf{b}_T, Q_0)$ is only designed to work in the large- b_T region, corresponding to low k_\perp

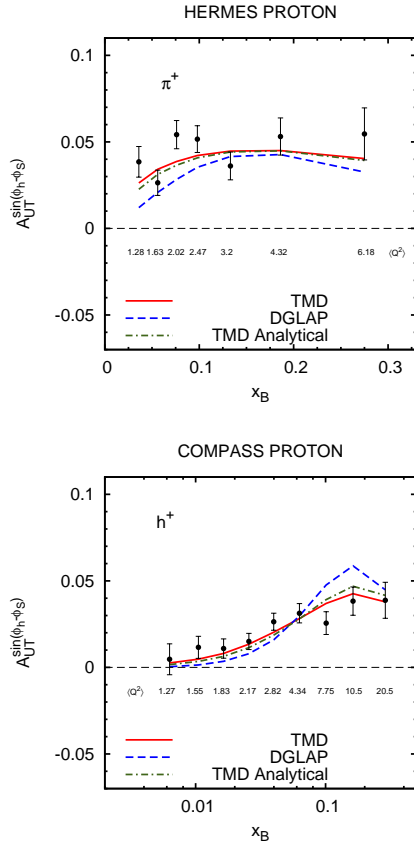


Fig. 8. The results obtained in Ref. [63] from the fit of the SIDIS $A_{UT}^{\sin(\phi_h - \phi_S)}$ asymmetries applying TMD evolution (red, solid lines) are compared with the analogous results found by using DGLAP evolution equations (blue, dashed lines). The experimental data are from HERMES [82] and COMPASS [83] Collaborations.

values. Therefore, this formalism is perfectly suitable for phenomenological applications in the kinematical region we are interested in, but the parameterization of the input function should be revised in the case one wishes to apply it to a wider range of transverse momenta, like higher Q^2 processes where perturbative corrections become important, as discussed in Sect. 2.1

The results obtained in Ref. [63] are shown in Fig. 8. They showed that the recently proposed Q^2 TMD evolution scheme can already be observed in the available SIDIS data on the Siverson asymmetry.

A definite statement resulting from this analysis is that the best fit of all SIDIS data on the Siverson asymmetry using TMD-evolution, when compared with the same analysis performed with the simplified DGLAP-evolution, exhibits a smaller value of the total χ^2 . Not only, but when analyzing the partial contributions to the total χ^2 value of the single subsets of data, one realizes that such a smaller value mostly originates from the large Q^2 COMPASS data, which are greatly affected by the TMD evo-

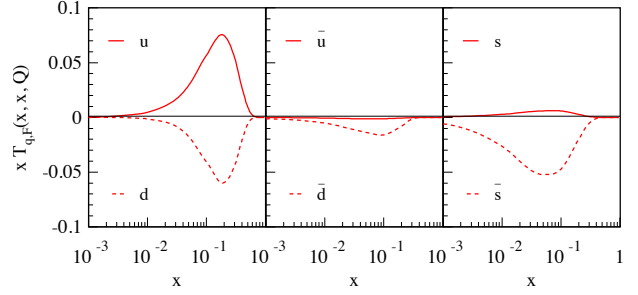


Fig. 9. The $T_{qF}(x, x, \mu)$ twist-three function as extracted in Ref. [87].

lution. This is indeed an indication in favor of the TMD evolution.

Later, an analogous phenomenological analysis, extended to Drell-Yan as well as SIDIS processes, was performed by Sun and Yuan [85], using an alternative, approximated form of the Sudakov form factor as proposed in Ref. [86]. Their study of TMD evolution effects in DY processes showed that extracting the free parameters which regulate the variation of the k_\perp shape of the Siverson function by fitting solely SIDIS experimental data, could induce a strong dilution of the DY asymmetries. As usual, special care should be used when blindly applying parameter values extracted from a process to a different one. In this case, for example, it turns out that Siverson SIDIS asymmetries are very little sensitive to the g_2 parameter, which fixes the Gaussian width of the g_K function, see Eq. (25), while the analogous asymmetries in DY are strongly affected by small variation of the same parameter. We conclude that global analyses, which include experimental data from as many different processes as possible, represent the only reliable strategies to reach the full picture of hadronic structure, including TMD evolution.

More recently, Echevarria et al. [87] have extracted the Siverson function using a CSS evolution scheme, but relating the first moment of the Siverson function to the twist-three Qiu-Sterman quark-gluon correlation function, $T_{qF}(x, x, \mu)$ [88]. The knowledge of $T_{qF}(x, x, \mu)$, i.e. the “collinear counterpart” of the Siverson function will be very important for the description of SSAs in pp scattering. The $T_{qF}(x, x, \mu)$ twist-three function, as extracted in Ref. [87], is presented in Fig. 9.

It is interesting to point out, here, that the Siverson function measured in SIDIS should be directly related to the twist-three Qiu-Sterman quark-gluon correlation function, $T_{qF}(x, x, \mu)$. It was noted, however, that the T_F extracted from SIDIS would give a single spin asymmetry A_N , in proton-proton scattering, with opposite sign with respect to that observed in experiments [89]. This observation is referred to as the “sign puzzle”. The attempts to solve this puzzle by considering the fact that kinematical regions of pp and SIDIS experiments are different, or by allowing the Siverson function to change sign, as a function of transverse momentum, did not result in a satisfactory solution of the problem. The more complete twist-3 phenomenology suggests [90] that fragmentation functions may play a more important role and generate the asymmetries in pp .

Future Drell-Yan experiments at COMPASS, RHIC and Fermilab are going to reveal both the sign and the evolution of the Sivers function with respect to SIDIS measurements. Dedicated studies of TMD phenomenology in DY processes [91,92,93] will then become of crucial importance. Notice that the GPM model predicts the same sign of Sivers function in DY and SIDIS, while analyses including gauge links and TMD factorizations [21,94] suggests that the sign will change in DY with respect to SIDIS.

The Gluon Sivers function will be important at EIC: dedicated studies can be found for example in Ref. [95].

2.3 Collins Function and Transversity

The transversity distribution h_1 is the only source of information on the tensor charge of the nucleon and the Collins FF H_1^\perp decodes the fundamental correlation between the transverse spin of a fragmenting quark and the transverse momentum of the final produced hadron.

The Collins fragmentation function can be studied in SIDIS experiments, where it appears convoluted with the transversity distribution, and where, being dependent on the hadronic intrinsic transverse momentum, it induces a typical azimuthal modulation, the Collins asymmetry. It can also induce azimuthal angular correlations between hadrons produced in opposite jets in e^+e^- annihilations: here two of such functions, corresponding to the two final hadrons, appear convoluted. Consequently, a simultaneous analysis of SIDIS and e^+e^- data allows the combined extraction of the transversity distribution and the Collins fragmentation functions [48,49,53]. Notice that this is made possible by the universality of fragmentation functions, soft factors, and parton densities between e^+e^- annihilation, semi-inclusive deep-inelastic scattering and the Drell-Yan process, which was proven in Refs. [96,97].

Recently, new data on the $e^+e^- \rightarrow h_1 h_2 X$ process have been published by the BaBar Collaboration, focusing on their z and p_\perp dependence [52]. It is the first direct measurement of the transverse momentum dependence of an asymmetry, in e^+e^- processes, related to TMD functions. Moreover, the newest results from BESIII [98], at much lower Q^2 values with respect to Belle and BaBar data, allow to explore the sensitivity of these azimuthal correlations on Q^2 dependent effects. A review of the experimental measurements involving the TMD fragmentation functions can be found in the contribution of Garzia and Giordano in this Topical Issue.

As mentioned in Sect. 1, work along these lines has been and is being done by several groups [53,54,55,56]. Here we will briefly report on the main achievements in the phenomenological extraction of the Collins and transversity functions and on their TMD evolution properties.

Collins asymmetries in SIDIS are generated by the convolution of the transversity function $\Delta_T q$ or h_1 and the Collins TMD FF $\Delta^N D_{h/q^\dagger}$ or H_1^\perp . The Torino and Amsterdam group notations for the Collins function, are related by [99]

$$\Delta^N D_{h/q^\dagger}(z, p_\perp) = (2p_\perp/zm_h) H_1^{\perp q}(z, p_\perp). \quad (36)$$

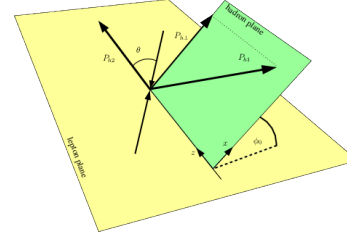


Fig. 10. Kinematical configuration and conventions for e^+e^- processes.

The relevant contributions to the SIDIS cross-sections are

$$\frac{d^5\sigma(S_\perp)}{dx_B dy dz_h d^2P_{h\perp}} = \sigma_0(x_B, y, Q^2) \left[F_{UU} + \sin(\phi_h + \phi_s) \frac{2(1-y)}{1+(1-y)^2} F_{UT}^{\sin(\phi_h + \phi_s)} + \dots \right]. \quad (37)$$

The polarized structure function $F_{UT}^{\sin(\phi_h + \phi_s)}$ contains the convolution of transversity with the Collins function, $h_1 \otimes H_1^\perp$. The Collins FFs generate azimuthal asymmetries in e^+e^- , where TMD factorization is appropriate, and read [100, 101]

$$\frac{d^5\sigma^{e^+e^- \rightarrow h_1 h_2 X}}{dz_{h1} dz_{h2} d^2P_{h\perp} d\cos\theta} = \frac{N_c \pi \alpha_{\text{em}}^2}{2Q^2} \left[(1 + \cos^2\theta) Z_{uu}^{h_1 h_2} + \sin^2\theta \cos(2\phi_0) Z_{\text{collins}}^{h_1 h_2} \right] \quad (38)$$

where θ is the polar angle between the hadron h_2 and the beam of e^+e^- , ϕ_0 is defined as the azimuthal angle of hadron h_1 relative to that of hadron h_2 , i.e. of the plane containing hadrons h_1 and h_2 relative to the plane containing hadron h_2 and the lepton pair (see Fig. 10), and $P_{h\perp}$ is the transverse momentum of hadron h_1 in this frame. The polarized structure function $Z_{\text{collins}}^{h_1 h_2}$ contains the convolution of two Collins functions, $H_1^\perp \otimes H_1^\perp$.

Two methods have been adopted in the experimental analysis of the Belle and BaBar data [50,52]:

- the “thrust-axis method” where the jet thrust axis, in the e^+e^- c.m. frame, fixes the \hat{z} direction and the $e^+e^- \rightarrow q\bar{q}$ scattering defines the $\hat{x}\hat{z}$ plane; φ_1 and φ_2 are the azimuthal angles of the two hadrons around the thrust axis, while θ is the angle between the lepton direction and the thrust axis
- the “hadronic-plane method”, in which one of the produced hadrons (h_2 in our case) identifies the \hat{z} direction and the $\hat{x}\hat{z}$ plane is determined by the lepton and the h_2 directions; the other relevant plane is determined by \hat{z} and the direction of the other observed hadron, h_1 , at an angle ϕ_1 with respect to the $\hat{x}\hat{z}$ plane. Here θ_2 is the angle between h_2 and the e^+e^- direction.

In this paper we will only discuss results obtained in the latter. In this reference frame, the elementary process $e^+e^- \rightarrow q\bar{q}$ does not occur in the $\hat{x}\hat{z}$ plane, and thus the

helicity scattering amplitudes involve an azimuthal phase φ_2 . Ratios of unlike/like and unlike/charged are built in order to avoid false asymmetries:

$$\frac{R_0^U}{R_0^{L(C)}} = 1 + \cos(2\phi_0) A_0^{UL(C)}, \quad (39)$$

which can then be directly compared to the experimental measurements. All details and definitions can be found in Ref. [56], which we will follow here.

For the unpolarised parton distribution and fragmentation functions the factorized forms of Eqs. (5) and (6) are assumed. For the transversity distribution, $\Delta_T q(x, k_\perp)$, and the Collins FF, $\tilde{\Delta}^N D_{h/q^\uparrow}(z, p_\perp)$, similar factorized shapes [48] are adopted:

$$\Delta_T q(x, k_\perp; Q^2) = \Delta_T q(x, Q^2) \frac{e^{-k_\perp^2 / \langle k_\perp^2 \rangle_T}}{\pi \langle k_\perp^2 \rangle_T}, \quad (40)$$

$$\tilde{\Delta}^N D_{h/q^\uparrow}(z, p_\perp; Q^2) = \tilde{\Delta}^N D_{h/q^\uparrow}(z, Q^2) h(p_\perp) \frac{e^{-p_\perp^2 / \langle p_\perp^2 \rangle}}{\pi \langle p_\perp^2 \rangle}, \quad (41)$$

where $\Delta_T q(x)$ is the integrated transversity distribution and $\tilde{\Delta}^N D_{h/q^\uparrow}(z)$ is the z -dependent part of the Collins function. In order to easily implement the proper positivity bounds, these functions are written, at the initial scale Q_0^2 , as [48]

$$\Delta_T q(x, Q_0^2) = \mathcal{N}_q^T(x, Q_0^2) \frac{1}{2} [f_{q/p}(x, Q_0^2) + \Delta q(x, Q_0^2)] \quad (42)$$

$$\tilde{\Delta}^N D_{h/q^\uparrow}(z, Q_0^2) = 2 \mathcal{N}_q^C(z, Q_0^2) D_{h/q}(z, Q_0^2). \quad (43)$$

They are then evolved up to the proper value of Q^2 . In Ref. [56], for $\Delta_T q(x, Q^2)$ we employ a transversity DGLAP kernel and the evolution is performed by an appropriately modified Hoppet code [102]; for the Collins function, Anselmino et al. assumed that the only scale dependence is contained in $D(z, Q^2)$, which is evolved with an unpolarised DGLAP kernel, while \mathcal{N}_q^C does not evolve with Q^2 . This is equivalent to assuming that the ratio $\tilde{\Delta}^N D(z, Q^2)/D(z, Q^2)$ is constant in Q^2 . The function $h(p_\perp)$, defined as [48]

$$h(p_\perp) = \sqrt{2e} \frac{p_\perp}{M_C} e^{-p_\perp^2 / M_C^2}, \quad (44)$$

allows for a possible modification of the p_\perp Gaussian width of the Collins function with respect to the unpolarised FF; for the TMD transversity distribution, instead, we assume the same Gaussian width as for the unpolarised TMD, $\langle k_\perp^2 \rangle_T = \langle k_\perp^2 \rangle$. In Ref. [56] a simplified model which implies no Q^2 dependence in the p_\perp distribution is used. We will compare the results obtained using this approximation with those presented in Ref. [103] using a NLL TMD evolution scheme for the Collins function.

$\mathcal{N}_q^T(x)$ is parameterized as

$$\mathcal{N}_q^T(x) = N_q^T x^\alpha (1-x)^\beta \frac{(\alpha+\beta)^{\alpha+\beta}}{\alpha^\alpha \beta^\beta} \quad (q = u_v, d_v) \quad (45)$$

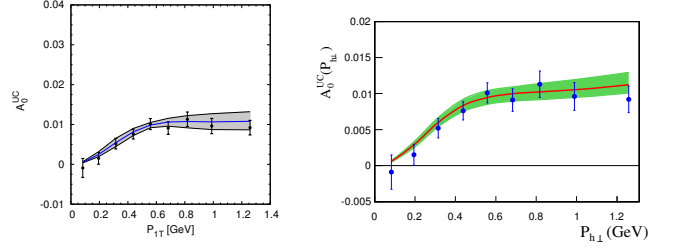


Fig. 11. The experimental data on the azimuthal correlations $A_0^{UL,C}$ as functions of P_{1T} in $e^+e^- \rightarrow h_1 h_2 X$ processes, as measured by the BaBar Collaboration [52], are compared to the curves obtained from a GPM model in Ref. [56] (left panel) and using NLL TMD evolution in Ref. [103] (right panel). The shaded areas correspond to the statistical uncertainty on the model parameters.

where $-1 \leq N_q^T \leq +1$, α and β are free parameters of the fit. Thus, the transversity distributions depend on a total of 4 parameters ($N_{u_v}^T, N_{d_v}^T, \alpha, \beta$). The Collins function, is distinguished in favoured and disfavoured contributions, parameterised as

$$\mathcal{N}_{\text{fav}}^C(z) = N_{\text{fav}}^C z^\gamma (1-z)^\delta \frac{(\gamma+\delta)^{\gamma+\delta}}{\gamma^\gamma \delta^\delta}, \quad \mathcal{N}_{\text{dis}}^C(z) = N_{\text{dis}}^C. \quad (46)$$

where $-1 \leq N_{\text{fav/dis}}^C \leq +1$, γ and δ are free parameters of the fit.

A best fit of the data on $A_{UT}^{\sin(\phi_h+\phi_S)}$ (HERMES and COMPASS) and of the data on $A_0^{UL,C}$ (Belle and BaBar) is then performed. It turns out to be a fit of excellent quality, with a total $\chi_{\text{d.o.f.}}^2 = 0.84$, equally good for SIDIS and e^+e^- data.

Let's focus on the new BaBar measurements of A_0^{UL} and A_0^{UC} asymmetries as functions of P_{1T} (p_{t0} in the notation used by the BaBar Collaboration). Fig. 11 shows our best fit of the BaBar A_0^{UL} and A_0^{UC} asymmetries as functions of P_{1T} . These data offer the first direct insight of the dependence of the Collins function on the parton intrinsic transverse momentum: in fact, global fits now deliver a more precise determination of the Gaussian width of the Collins function (through the M_C parameter), which in previous fits was affected by a very large uncertainty. Fig. 11 shows the best fit of the BaBar A_0^{UL} and A_0^{UC} asymmetries as functions of P_{1T} , as obtained in Ref. [56]. All details on the analysis and the values of the extracted parameters can be found there.

As shown in the left panel of Fig. 12, the u and d quark transversity functions extracted in Ref. [56] are compatible with the previous extractions [48,49,53], and with those obtained by a similar procedure, but involving the di-hadron fragmentation functions instead of the Collins function [57,58,59]. While the u valence transversity distribution has a clear trend, the d valence transversity still shows large uncertainties. Instead, the newly extracted Collins functions look different from those obtained in our previous analyses: this is mainly due to the fact that a different parameterisation for the disfavoured Collins function was exploited. This study indicates that the actual

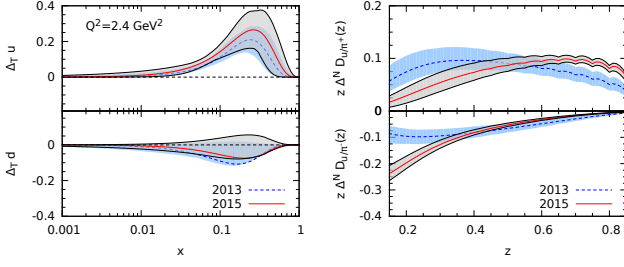


Fig. 12. Comparison of the best fit results obtained by Anselmino et al. in Ref. [56] (red, solid lines) for the valence u and d quark transversity distributions (left panel) and for the lowest p_\perp moment of the favoured and disfavoured Collins functions (right panel), at $Q^2 = 2.4 \text{ GeV}^2$, with those from their previous analysis [53] (blue, dashed lines).

shape of the disfavoured Collins function is still largely unconstrained by data. About the p_\perp dependence of the Collins function, we have already mentioned that its Gaussian width can now be determined with remarkable precision. However, this extraction is still subject to a number of initial assumptions: a Gaussian shape for the TMDs, a complete separation between transverse and longitudinal degrees of freedom, a Gaussian width of the unpolarised TMD-FFs fixed solely by SIDIS data. Hopefully, higher statistics and higher precision multidimensional data, for asymmetries and unpolarised multiplicities, will help clarifying the picture.

The first extraction of the transversity distribution and Collins fragmentation functions with TMD evolution was performed in Ref. [103]. It was demonstrated that the TMD evolution can describe the experimental data and constrain the nucleon tensor charge with improved theoretical accuracy. To achieve that, the most recent developments from both theory and phenomenology sides [10, 104, 105, 106, 79, 107, 108, 87, 109, 69] were used, and the TMD evolution at NLL order within the Collins-Soper-Sterman (CSS) [8, 9] formalism was applied to the data.

Applying the TMD evolution, F_{UU} and F_{UT} can be written as [8, 9, 110, 106]

$$F_{UU} = \frac{1}{z_h^2} \int \frac{db b}{2\pi} J_0\left(\frac{P_{h\perp} b}{z_h}\right) e^{-S_{\text{PT}}(Q, b_*) - S_{\text{NP}}^{(\text{SIDIS})}(Q, b)} \times C_{q \leftarrow i} \otimes f_1^i(x_B, \mu_b) \hat{C}_{j \leftarrow q}^{(\text{SIDIS})} \otimes \hat{D}_{h/j}(z_h, \mu_b), \quad (47)$$

$$F_{UT} = -\frac{1}{2z_h^3} \int \frac{db b^2}{2\pi} J_1\left(\frac{P_{h\perp} b}{z_h}\right) e^{-S_{\text{PT}}(Q, b_*) - S_{\text{NP coll}}^{(\text{SIDIS})}(Q, b)} \times \delta C_{q \leftarrow i} \otimes h_1^i(x_B, \mu_b) \delta \hat{C}_{j \leftarrow q}^{(\text{SIDIS})} \otimes \hat{H}_{h/j}^{(3)}(z_h, \mu_b), \quad (48)$$

where b is the Fourier conjugate variable to the measured final hadron momentum $P_{h\perp}$, J_1 is the Bessel function, $\mu_b = c_0/b_*$ with $c_0 \simeq 1.12$, and the symbol \otimes represents the usual convolution in momentum fractions. The sum over quark flavors q weighted with quark charge, $\sum_q e_q^2$,

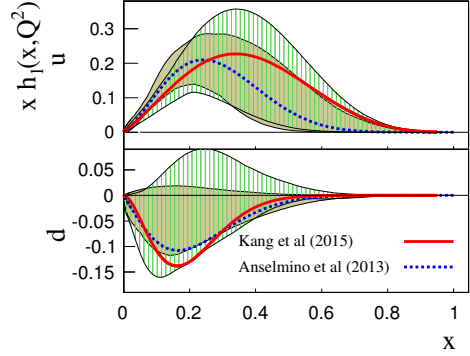


Fig. 13. Transversity distribution for up and down quarks comparison of extraction in Ref. [103] and [53]. The band corresponds to the uncertainty of the extraction.

and the sum over $i, j = q, \bar{q}, g$, are implicit in all formulas for the structure functions. C , \hat{C} and δC , $\delta \hat{C}$ are the coefficient functions for the unpolarized distribution and fragmentation functions, and for transversity and Collins FF, that can be calculated perturbatively.

The usual b_* -prescription was used in Ref. [103] and non perturbative factors were introduced $S_{\text{NP}}^{(\text{SIDIS})}$ and $S_{\text{NP coll}}^{(\text{SIDIS})}$ that contain information on the initial conditions of evolution. The Collins fragmentation function [18] enters as a p_\perp moment [104],

$$\hat{H}_{h/q}^{(3)}(z_h) = \int d^2 p_\perp \frac{|p_\perp^2|}{M_h} H_{1h/q}^\perp(z_h, p_\perp), \quad (49)$$

where $H_{1h/q}^\perp(z_h, p_\perp)$ is the quark Collins function defined in [104], and differs by a factor $(-1/z_h)$ from the so-called ‘‘Trento convention’’ [99],

$$H_{1h/j}^\perp(z_h, p_\perp) = -\frac{1}{z_h} H_{1h/j}^\perp(z_h, p_\perp)|_{\text{Trento}}, \quad (50)$$

with p_\perp the transverse component of the hadron with respect to the fragmenting quark momentum.

Three important ingredients have to be included to achieve the NLL formalism for the above structure functions and asymmetries. First of all, the perturbative Sudakov form factor [111],

$$S_{\text{PT}}(Q, b_*) = \int_{\mu_b^2}^{Q^2} \frac{d\mu^2}{\mu^2} \left[A \ln \frac{Q^2}{\mu^2} + B \right], \quad (51)$$

with perturbative coefficients $A^{(1,2)} \sim \alpha_s^{(1,2)}$ and $B^{(1)} \sim \alpha_s^1$ [112, 111]. Then, the scale evolutions of the quark transversity distribution and of the Collins fragmentation functions up to the scale of μ_b .

The global fit of SIDIS and e^+e^- was performed and resulted in the total $\chi^2/n_{d.o.f} = 0.88$, equally good for SIDIS and e^+e^- data. A plot showing the results obtained in Ref. [103] is presented in Fig. 11 (left panel), where they are compared with the results obtained in Ref. [56]. It is

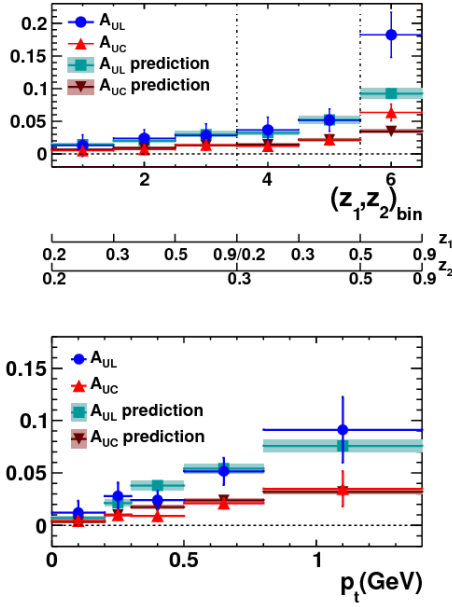


Fig. 14. Predictions using results of Ref. [54, 103] and comparison to A_0^{UC} (upper panel) and A_0^{UL} (bottom panel) asymmetries measured by the BESIII collaboration [98] at $Q^2 = 13 \text{ GeV}^2$. Plot from Ref. [98]

very interesting to notice the strong similarity between the two curves obtained with and without evolution. As the asymmetries measured by BaBar and Belle are actually double ratios, this similarity might be an indication of possible cancellations of strong evolution effects between numerators and denominators.

Fig. 13 shows the comparison of the results from [103] and [53]. The right panel of Fig. 13 shows the predictions for future measurements at an EIC.

The BESIII Collaboration has recently measured the $\cos 2\phi_0$ asymmetries observed by BaBar and Belle, but at the lower energy $\sqrt{s} = Q = 3.65 \text{ GeV}$ [98], see Fig. 14. Their low Q^2 values, as compared with Belle and BaBar experiments, might help in assessing the importance of TMD evolution effects. It is therefore important to check how a model in which the Q^2 dependence of the TMD Gaussian width is not included [56] can describe these new sets of measurements, and compare these results with the description obtained by using a TMD evolution scheme [103]. In Fig. 15 the solid, black circles represent the A_0^{UC} and A_0^{UL} asymmetries measured by the BESIII Collaboration at $Q^2 = 13 \text{ GeV}^2$, in bins of (z_1, z_2) , while the solid blue circles (with their relative bands) correspond to the predictions obtained by using the results of Ref. [56]. These asymmetries are well reproduced at small z_1 and z_2 , where we expect our model to work, while they are underestimated at very large values of either z_1 or z_2 , or both. Notice that the values of z_1, z_2 in the last bins are very large for an experiment with $\sqrt{s} = 3.65 \text{ GeV}$: such data points might be affected by exclusive production contributions, and other effects. Fig. 14 shows the predictions for the BESIII asymmetries obtained in Ref. [103], evolving the

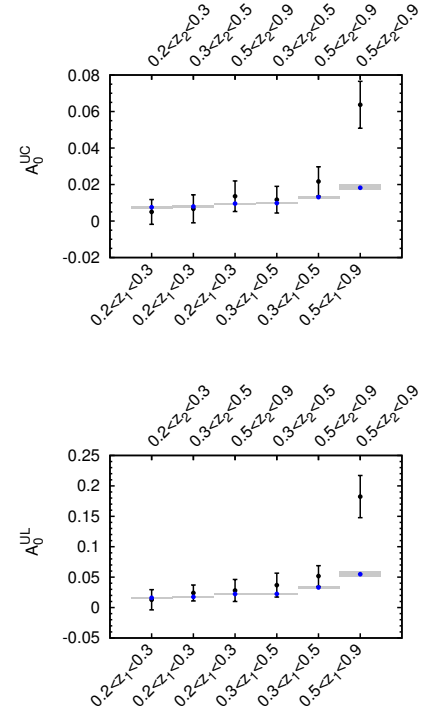


Fig. 15. The solid, black circles represent the A_0^{UC} (left panel) and A_0^{UL} (right panel) asymmetries measured by the BESIII collaboration [98] at $Q^2 = 13 \text{ GeV}^2$, in bins of (z_1, z_2) , while the solid blue circles (with their relative bands) correspond to the predictions obtained by using the Collins functions from our alternative fit.

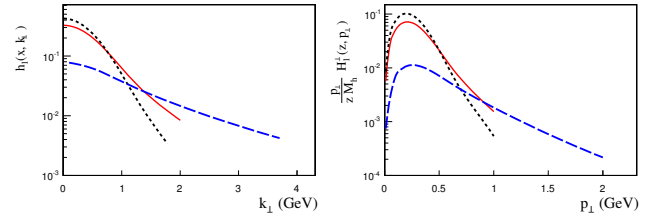


Fig. 16. Transversity distribution h_1 (left panel) and Collins fragmentation function H_1^\perp (right panel) at three different scales $Q^2 = 2.4, 10, 1000 \text{ GeV}^2$ (solid, dotted, and dashed lines). The plots are from Ref. [103]

Collins function with a TMD equations. As in the previous case, there is a striking similarity with the predictions obtained in Ref. [56] with no TMD evolution (which gives almost identical asymmetries for different Q^2).

The transversity distribution and the Collins FF, as extracted in Ref. [103], are shown in Fig. 16 as function of k_\perp and p_\perp at three different Q^2 scales. The typical broadening dilution of the curves as Q^2 increases is clearly visible. Note that Ref. [103] obtained quite slow a TMD evolution in the low Q^2 range by re-extracting the appropriate non perturbative kernel of TMD evolution for the data.

At this stage, it is quite difficult to draw any clear-cut conclusion: despite the sizeable difference in Q^2 among the different sets of e^+e^- data differences among the measured BESIII and BaBar-Belle asymmetries are mild and can be explained by the different kinematical configurations and cuts. Predictions obtained with and without TMD evolution are both in qualitatively good agreement with the present BESIII measurements, indicating that the data themselves do not show strong sensitivity to the Q^2 dependence in the transverse momentum distribution.

Effects of TMD evolution in e^+e^- annihilation into hadrons were recently studied in Ref [55].

2.4 Boer-Mulders function

The Boer-Mulder function [113], $\Delta f_{q^\uparrow/p}$ or h_1^\perp in the Torino or Amsterdam notation respectively, measures the transverse polarization asymmetry of quarks inside an unpolarized nucleon. It can be extracted by analyzing the $\cos\phi$ and $\cos 2\phi$ azimuthal modulations that appear in the unpolarized SIDIS cross section, see Eq. (1). The structure function associated with the $\cos\phi$ modulation turns out to be of order $1/Q$. Neglecting the dynamical twist-3 contributions (the so-called “tilde” TMD functions, which arise from quark-gluon correlations), $F_{UU}^{\cos\phi}$ can be written as the sum of two terms

$$F_{UU}^{\cos\phi} = F_{UU}^{\cos\phi}\Big|_{\text{Cahn}} + F_{UU}^{\cos\phi}\Big|_{\text{BM}}, \quad (52)$$

with $(\mathbf{h} \equiv \mathbf{P}_T/|\mathbf{P}_T|)$

$$F_{UU}^{\cos\phi}\Big|_{\text{Cahn}} = -2 \sum_q e_q^2 x \int d^2\mathbf{k}_\perp \frac{(\mathbf{k}_\perp \cdot \mathbf{h})}{Q} f_q(x, k_\perp) D_q(z, p_\perp), \quad (53)$$

$$F_{UU}^{\cos\phi}\Big|_{\text{BM}} = \sum_q e_q^2 x \int d^2\mathbf{k}_\perp \frac{k_\perp}{Q} \frac{P_T - z(\mathbf{k}_\perp \cdot \mathbf{h})}{k_\perp} \otimes \Delta f_{q^\uparrow/p}(x, k_\perp) \Delta D_{h/q^\uparrow}(z, p_\perp). \quad (54)$$

Eq. (53) is the Cahn term, which accounts for the non-collinear kinematics of quarks in the elementary subprocess $\ell q \rightarrow \ell' q'$. Eq. (54) is the Boer-Mulders contribution, arising from the correlation between the transverse spin and the transverse momentum of quarks inside the unpolarized proton. In this term the Boer-Mulders distribution function $\Delta f_{q^\uparrow/p}$ couples to the Collins fragmentation function $\Delta D_{h/q^\uparrow}$. The relations between these functions, as defined in the present paper, and the corresponding quantities in the Amsterdam notation is

$$\Delta f_{q^\uparrow/p}(x, k_\perp) = -\frac{k_\perp}{M_p} h_1^\perp(x, k_\perp), \quad (55)$$

$$\Delta D_{h/q^\uparrow}(z, p_\perp) = \frac{2p_\perp}{zM_h} H_1^\perp(z, p_\perp), \quad (56)$$

where M_p and M_h are the masses of the proton and of the final hadron, respectively. The Boer-Mulders effect is also responsible of the $\cos 2\phi$ modulation of the cross section, giving a leading-twist contribution (that is, unsuppressed in Q), which has the form

$$F_{UU}^{\cos 2\phi}\Big|_{\text{BM}} = - \sum_q e_q^2 x \int d^2\mathbf{k}_\perp \frac{P_T(\mathbf{k}_\perp \cdot \mathbf{h}) + z_h [k_\perp^2 - 2(\mathbf{k}_\perp \cdot \mathbf{h})^2]}{2k_\perp p_\perp} \times \Delta f_{q^\uparrow/p}(x, k_\perp) \Delta D_{h/q^\uparrow}(z, p_\perp). \quad (57)$$

The $\cos\phi$ and $\cos 2\phi$ asymmetries are given, in terms of the structure functions, by

$$A^{\cos\phi} = \frac{2(2-y)\sqrt{1-y}}{[1+(1-y)^2]} \frac{F_{UU}^{\cos\phi}}{F_{UU}}, \quad (58)$$

$$A^{\cos 2\phi} = \frac{2(1-y)}{[1+(1-y)^2]} \frac{F_{UU}^{\cos 2\phi}}{F_{UU}}. \quad (59)$$

Up to order $1/Q$, $\langle \cos\phi \rangle$ receives contributions from the Cahn and the Boer-Mulders effect, while $\langle \cos 2\phi \rangle$ is proportional to the sole Boer-Mulders effect:

$$A^{\cos\phi} = A^{\cos\phi}\Big|_{\text{Cahn}} + A^{\cos\phi}\Big|_{\text{BM}}$$

$$A^{\cos 2\phi} = A^{\cos 2\phi}\Big|_{\text{BM}}$$

A few years ago, these azimuthal asymmetries in unpolarized SIDIS were measured by the COMPASS and HERMES Collaborations for positive and negative hadrons, and presented as one-dimensional projections, with all variables (x_B, z_h, Q^2, P_T) but one integrated over [114,115,116]. The one-dimensional data on the $\cos 2\phi$ asymmetry were analyzed in Ref. [117], where it was shown that the larger asymmetry for $\pi^- (h^-)$ production, compared to $\pi^+ (h^+)$, was an indication of the existence of a non-zero Boer-Mulders effect, in agreement with the earlier predictions of Ref. [118]. Moreover, the analysis of Ref. [117] revealed that both up and down-quark Boer-Mulders functions are negative, see Fig. 17, consistently with various theoretical expectations (impact-parameter approach [119], lattice results [120], large- N_c predictions [121] and model calculations [122,123,124]. It was also pointed out that measurements at different values of Q^2 were essential, in order to disentangle higher-twist contributions from the twist-two Boer-Mulder term.

The HERMES and COMPASS Collaborations have recently provided multidimensional data in bins of x_B , z_h , Q^2 and P_T for the multiplicities [40,41] and for the azimuthal asymmetries [39,44]. A study of the SIDIS azimuthal moments $\langle \cos\phi \rangle$ and $\langle \cos 2\phi \rangle$ was presented by Barone et al. in Ref. [45], in order to understand the role of the Cahn effect and to extract the Boer-Mulders function, which was parameterized as follows

$$\Delta f_{q^\uparrow/p}(x, k_\perp) = \Delta f_{q^\uparrow/p}(x) \sqrt{2e} \frac{k_\perp}{M_{\text{BM}}} \frac{e^{-k_\perp^2/\langle k_\perp^2 \rangle_{\text{BM}}}}{\pi \langle k_\perp^2 \rangle_{\text{BM}}}, \quad (60)$$

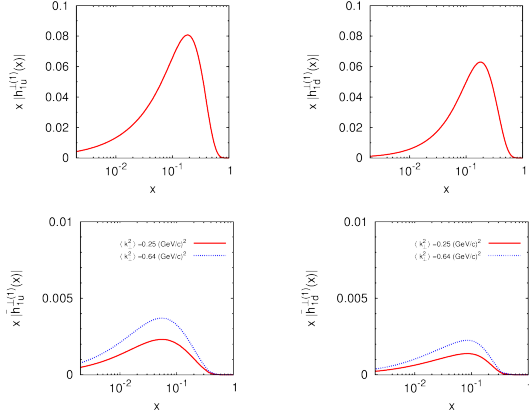


Fig. 17. First moment of the Boer-Mulders distribution for up and down-quarks (left panel) and for anti-up and anti-down quarks (right panel) at $Q^2 = 2.4 \text{ GeV}^2$. These plots are from Refs. [117,125].

with

$$\Delta f_{q^+ / p}(x) = N_q f_{q/p}(x), \quad (61)$$

and

$$\langle k_{\perp}^2 \rangle_{\text{BM}} = \frac{\langle k_{\perp}^2 \rangle M_{\text{BM}}^2}{\langle k_{\perp}^2 \rangle + M_{\text{BM}}^2}. \quad (62)$$

N_q and M_{BM} are free parameters to be determined by the fit. For the favored and the disfavored components of the Collins function, the parameters are fixed to the values obtained in a recent fit of the Collins asymmetries in SIDIS and e^+e^- annihilation [53], as described in Sect. 2.3.

F_{UU} and the Cahn contribution to $\langle \cos \phi \rangle$ involve only the unpolarized TMD distribution and fragmentation functions $f_{q/p}(x, k_{\perp})$ and $D_{h/q}(z, p_{\perp})$. These functions have been recently extracted in Ref. [43], as described Sect. 2.1. There it was observed that, since the multiplicities are sensitive only to the combination $\langle P_T^2 \rangle = z_h^2 \langle k_{\perp}^2 \rangle + \langle p_{\perp}^2 \rangle$, Eq. (7), they cannot distinguish $\langle k_{\perp}^2 \rangle$ from $\langle p_{\perp}^2 \rangle$. Instead, the azimuthal asymmetries involve $\langle k_{\perp}^2 \rangle$ and $\langle p_{\perp}^2 \rangle$ separately, and are sensitive to a z_h -dependent $\langle p_{\perp}^2 \rangle$. Therefore, in principle, by fitting simultaneously the multiplicities and the $\cos \phi$ and $\cos 2\phi$ asymmetries one should be able to extract the separate values of $\langle k_{\perp}^2 \rangle$ and $\langle p_{\perp}^2 \rangle$.

Unfortunately, the analysis of Ref. [45] shows that, due to the huge contribution of the Cahn effect, the recent COMPASS and HERMES multidimensional data can only be reproduced by a very small value of $\langle k_{\perp}^2 \rangle$, namely $0.03\text{--}0.04 \text{ GeV}^2$. This means that most of the transverse momentum of the outgoing hadron is due to the fragmentation, which must be described by a function with a z -dependent width. This result, mainly driven by $\langle \cos \phi \rangle$, could be modified by the presence of further twist-3 terms, which might not be negligible due to the relevance of the small- Q^2 region in the present measurements.

A somehow disappointing output of this fits is the indeterminacy on the extraction of the Boer-Mulders function, which seems to play a minor role in the asymmetries. This is seen in particular from $\langle \cos 2\phi \rangle$, which is entirely deter-

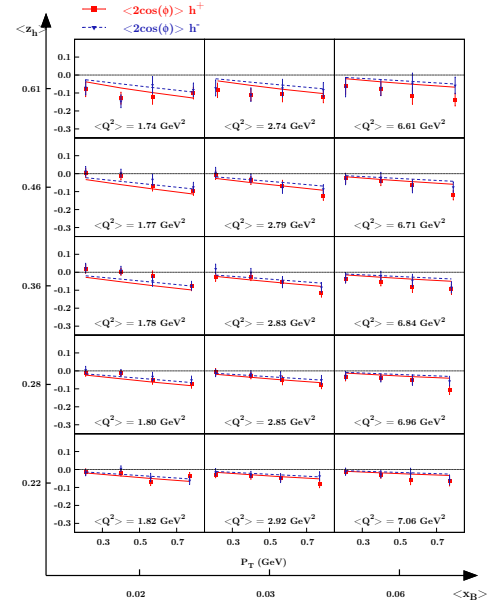


Fig. 18. Best fit curves for $\langle \cos \phi \rangle$ obtained by fitting COMPASS multiplicities, $\langle \cos \phi \rangle$ and $\langle \cos 2\phi \rangle$ data. The Cahn effect in $\langle \cos 2\phi \rangle$ has been set to zero. Plot from Ref. [45].

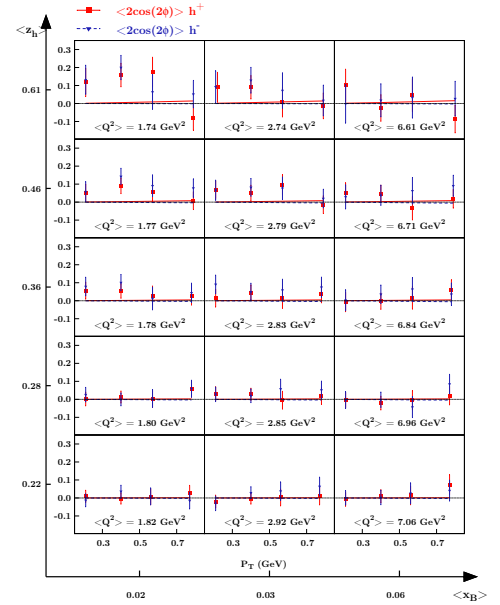


Fig. 19. Best fit curves for $\langle \cos 2\phi \rangle$ obtained by fitting COMPASS multiplicities, $\langle \cos \phi \rangle$ and $\langle \cos 2\phi \rangle$ data. The Cahn effect in $\langle \cos 2\phi \rangle$ has been set to zero. Plot from Ref. [45].

mined by the Boer-Mulders contribution but appears to be, within large errors, compatible with zero.

On the other hand, the integrated $\langle \cos 2\phi \rangle$ data [44] show a non vanishing asymmetry, especially when plotted against z . The asymmetry is positive for π^+ and negative for π^- , as expected from the Boer-Mulders effect [118]. Also the integrated data on $\langle \cos \phi \rangle$ show a different asymmetry for π^+ and π^- (negative in the first case, positive in the other): this indicates a flavor dependence which

can only be achieved with a non-zero Boer-Mulders effect since, within a flavor-independent Gaussian model with factorized x and k_\perp dependences, the Cahn effect is flavor blind and can only generate identical contributions for positively or negatively charged pions. However, the sign of the u and d Boer-Mulders functions required for a successful description of $\langle \cos 2\phi \rangle$ appears to be incompatible with those required to generate the appropriate difference between π^+ and π^- in the $\langle \cos \phi \rangle$ azimuthal moment. Unfortunately, not even a more refined model with flavor dependent Gaussian widths can help, given the precision of the current experimental data.

One should not forget about the existence of other higher-twist effects that could combine with the Boer-Mulders term and alter the simple picture considered here. In order to disentangle these contributions, it might be useful to integrate the asymmetry data on restricted kinematical ranges, as suggested in Ref. [126], so as to avoid the low- Q^2 region and meet the requirements of TMD factorization. Analyzing properly integrated data could help to clarify the origin of azimuthal asymmetries and possibly to get more information on the Boer-Mulders function.

The Boer-Mulders functions also generate the $\cos(2\phi_h)$ asymmetry in Drell-Yan processes: this asymmetry is proportional to the convolution of the Boer-Mulders functions for quark and for anti-quark $h_1^\perp \otimes \bar{h}_1^\perp$. In Ref. [125] the anti-quark Boer-Mulders distributions were extracted using the E866/NuSea measurements of pp and pD unpolarized DY [127, 128]. Possible effects of TMD evolution were also studied in Ref. [125], by varying the width of the functions. (solid red and dashed blue curves in Fig. 17).

Future developments will involve studies of the Boer-Mulders functions including TMD evolution effects.

2.5 Pretzelosity

The pretzelosity distribution function h_{1T}^\perp [129] describes transversely polarized quarks inside a transversely polarized nucleon.

The part of the SIDIS cross section we are interested in reads [130, 131, 84]:

$$\frac{d^5\sigma(S_\perp)}{dx_B dy dz_h d^2P_{h\perp}} = \sigma_0(x_B, y, Q^2) \left[F_{UU} + \sin(3\phi_h - \phi_s) \frac{2(1-y)}{1+(1-y)^2} F_{UT}^{\sin(3\phi_h - \phi_s)} + \dots \right], \quad (63)$$

where the spin structure function $F_{UT}^{\sin(3\phi_h - \phi_s)}$ contains the convolution of pretzelosity h_{1T}^\perp and the Collins FF H_1^\perp .

Pretzelosity is the only TMD distribution that gives a quadrupole modulation of the parton densities in the momentum space, as shown in Fig. 21.

The measured asymmetry in SIDIS contains the convolution of pretzelosity h_{1T}^\perp and the Collins FF H_1^\perp :

$$A_{UT}^{\sin(3\phi_h - \phi_s)} \equiv \langle 2 \sin(3\phi_h - \phi_s) \rangle \sim \frac{h_{1T}^\perp \otimes H_1^\perp}{f_1 \otimes D_1}. \quad (64)$$

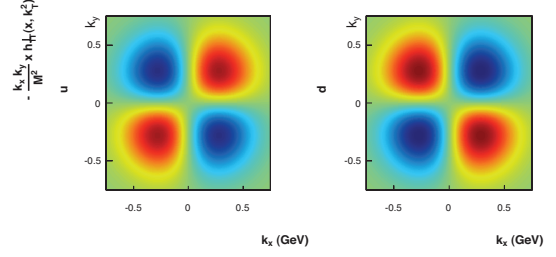


Fig. 20. Tomographic slice of the pretzelosity distribution at $x = 0.1$ for up and down quarks. The plot is from Ref. [129]

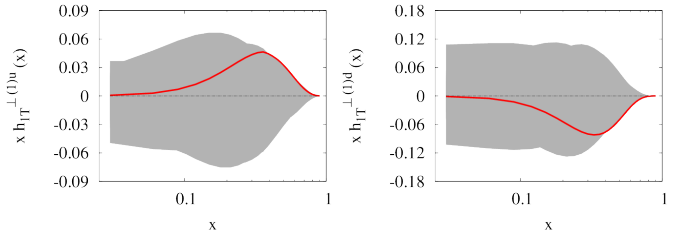


Fig. 21. First moment of the pretzelosity distribution for up (left panel) and down (right panel) quarks at $Q^2 = 2.4 \text{ GeV}^2$. The plot is from Ref. [129]

Notice that the knowledge of the Collins FF is needed for the extraction of pretzelosity. h_{1T}^\perp was extracted in Ref. [129]: the results are shown in Fig. 21. Notice that the current knowledge of pretzelosity is very poor due to the suppression of this asymmetry by kinematical factors. Future data from Jefferson Lab will be crucial for the phenomenology of h_{1T}^\perp .

In a vast class of models with spherically symmetric nucleon wave function in the rest frame, the pretzelosity distribution is related to the orbital angular momentum of quarks by the following relation

$$\mathcal{L}_z^a = - \int dx d^2\mathbf{k}_\perp \frac{k_\perp^2}{2M^2} h_{1T}^{\perp a}(x, k_\perp^2) = - \int dx h_{1T}^{\perp(1)a}(x). \quad (65)$$

Even though the relation of Eq. 65 is indeed model dependent, it is interesting to explore it to gain more information on this effect.

2.6 Future

In the last few decades it was realized that a simple *collinear* picture of the nucleon, with partons that move along the direction of motion of the nucleon itself, and encode parton dynamics into the parton distribution and fragmentation functions, is not sufficient to explain all phenomena associated with the nucleon's structure. The explanation of large Spin Asymmetries, early observed in hadronic reactions and later in SIDIS and in e^+e^- annihilation processes, requires taking into account the transverse motion of partons with respect to the parent nucleon motion. This leads to the exploration of the three dimensional structure of the nucleon, which brings our knowledge of nuclear structure to a new and deeper level.

Correlations between spin and partonic intrinsic transverse momentum are encoded in the TMDs, transverse momentum dependent structure functions which play a fundamental role in unraveling the non-perturbative aspects of the hadronic structure of matter.

Having reviewed the state-of-the-art of TMD phenomenology, we give a brief summary of the forthcoming events which are presently foreseen in this field.

With HERMES data analyses being officially closed, and the COMPASS experiment entering phase 2, with the DY program, the flow of novel SIDIS data will rely on the last analyses and re-analysis of COMPASS data now on tape (2010-2012 data takings) and on the upgrade of the Jefferson Lab experiments from 6 to 12 GeV.

The Jefferson Lab 12 GeV program is going to explore the region of relatively high- x dominated by valence quarks. The description of the data will require a very good understanding of the non perturbative effects and of the kinematical corrections, such as phase space limitations and target mass corrections. Clearly, phenomenological studies of the non-perturbative TMD functions will be very important for the description of Jefferson Lab new data.

RHIC [23], COMPASS [22] and Fermilab [24] will provide data on polarized Drell-Yan and one will be able to incorporate these data in global analyses and investigate issues like the change of sign of the Sivers function [21], the flavour dependence of TMDs and eventual flavour asymmetries in the light quark sea. In particular, data on proton-proton scattering asymmetries from RHIC will be very important for TMD and twist-3 phenomenology [23,90]. The “sign” puzzle [89] will most probably be solved in future.

Future Electron Ion Collider will explore the region dominated by sea quarks and gluons and the data will provide a unique opportunity to study both sea quark and gluon TMDs and to study the evolution of asymmetries and TMDs [72]. For a detailed report on the future of TMDs (and GPDs) we refer the reader to the contribution of R. Ent to this Topical issue.

Finally, the Large Hadron Collider is going to provide an unprecedented amount of data relevant to three dimensional nucleon structure studies. Both gluon TMDs and quark TMDs will be important for LHC studies.

Combined studies from all facilities will result in the ultimate understanding of the mechanisms and the origin of spin asymmetries and will lead to a more profound knowledge of the origin of spin and the 3D nucleon structure.

We are grateful to S. Melis and J.O. Gonzalez H. for useful discussions and for revising the final version of this review. M.B. acknowledges the support of “Progetto di Ricerca Ate-neo/CSP” (codice TO-Call3-2012-0103).

References

1. R. P. Feynman, R. D. Field, and G. C. Fox. Correlations Among Particles and Jets Produced with Large Trans-

- verse Momenta. *Nucl. Phys.*, B128:1–65, 1977.
2. R. P. Feynman, R. D. Field, and G. C. Fox. A Quantum Chromodynamic Approach for the Large Transverse Momentum Production of Particles and Jets. *Phys. Rev.*, D18:3320, 1978.
3. Howard Georgi and H. David Politzer. Clean Tests of QCD in μp Scattering. *Phys. Rev. Lett.*, 40:3, 1978.
4. A. Mendez. QCD Predictions for Semiinclusive and Inclusive Leptoproduction. *Nucl. Phys.*, B145:199, 1978.
5. Gordon L. Kane, J. Pumplin, and W. Repko. Transverse Quark Polarization in Large $p(T)$ Reactions, $e^+ e^-$ Jets, and Leptoproduction: A Test of QCD. *Phys. Rev. Lett.*, 41:1689, 1978.
6. Robert N. Cahn. Azimuthal Dependence in Leptoproduction: A Simple Parton Model Calculation. *Phys. Lett.*, B78:269, 1978.
7. R. N. Cahn. Critique of Parton Model Calculations of Azimuthal Dependence in Leptoproduction. *Phys. Rev.*, D40:3107–3110, 1989.
8. John C. Collins and Davison E. Soper. Back-To-Back Jets in QCD. *Nucl. Phys.*, B193:381, 1981. [Erratum: *Nucl. Phys.* B213,545(1983)].
9. John C. Collins, Davison E. Soper, and George F. Sterman. Transverse Momentum Distribution in Drell-Yan Pair and W and Z Boson Production. *Nucl. Phys.*, B250:199, 1985.
10. John Collins. *Foundations of perturbative QCD*. Cambridge University Press, 2013.
11. A. V. Efremov and O. V. Teryaev. On Spin Effects in Quantum Chromodynamics. *Sov. J. Nucl. Phys.*, 36:140, 1982. [*Yad. Fiz.* 36,242(1982)].
12. A. V. Efremov and O. V. Teryaev. The Transversal Polarization in Quantum Chromodynamics. *Sov. J. Nucl. Phys.*, 39:962, 1984. [*Yad. Fiz.* 39,1517(1984)].
13. Jian-wei Qiu and George F. Sterman. Single transverse spin asymmetries. *Phys. Rev. Lett.*, 67:2264–2267, 1991.
14. Jian-wei Qiu and George F. Sterman. Single transverse spin asymmetries in hadronic pion production. *Phys. Rev.*, D59:014004, 1999.
15. Xiangdong Ji, Jian-Wei Qiu, Werner Vogelsang, and Feng Yuan. A Unified picture for single transverse-spin asymmetries in hard processes. *Phys. Rev. Lett.*, 97:082002, 2006.
16. Dennis W. Sivers. Single spin production asymmetries from the hard scattering of point - like constituents. *Phys. Rev.*, D41:83, 1990.
17. Dennis W. Sivers. Hard scattering scaling laws for single spin production asymmetries. *Phys. Rev.*, D43:261–263, 1991.
18. John C. Collins. Fragmentation of transversely polarized quarks probed in transverse momentum distributions. *Nucl. Phys.*, B396:161–182, 1993.
19. Stanley J. Brodsky, Dae Sung Hwang, and Ivan Schmidt. Initial state interactions and single spin asymmetries in Drell-Yan processes. *Nucl. Phys.*, B642:344–356, 2002.
20. Stanley J. Brodsky, Dae Sung Hwang, and Ivan Schmidt. Final state interactions and single spin asymmetries in semi-inclusive deep inelastic scattering. *Phys. Lett.*, B530:99–107, 2002.
21. John C. Collins. Leading twist single transverse-spin asymmetries: Drell-Yan and deep inelastic scattering. *Phys. Lett.*, B536:43–48, 2002.

22. F. Gautheron et al. COMPASS-II Proposal. 2010, <https://wwwcompass.cern.ch/compass/publications>.
23. Elke-Caroline Aschenauer et al. The RHIC SPIN Program: Achievements and Future Opportunities. 2015.
24. L. D. Isenhower et al. Polarized Drell-Yan measurements with the Fermilab Main Injector. 2012.
25. M. Anselmino, Mariaelena Boglione, and F. Murgia. Single spin asymmetry for $pp^\uparrow \rightarrow \pi X$ in perturbative QCD. *Phys. Lett.*, B362:164–172, 1995.
26. M. Anselmino, M. Boglione, and F. Murgia. Phenomenology of single spin asymmetries $pp^\uparrow \rightarrow \pi X$. *Phys. Rev.*, D60:054027, 1999.
27. M. Boglione and E. Leader. Reassessment of the Collins mechanism for single spin asymmetries and the behavior of Delta $d(x)$ at large x . *Phys. Rev.*, D61:114001, 2000.
28. M. Anselmino, M. Boglione, U. D'Alesio, E. Leader, and F. Murgia. Accessing Sivers gluon distribution via transverse single spin asymmetries in $pp^\uparrow \rightarrow \pi X$ processes at RHIC. *Phys. Rev.*, D70:074025, 2004.
29. M. Anselmino, M. Boglione, U. D'Alesio, E. Leader, S. Melis, and F. Murgia. The general partonic structure for hadronic spin asymmetries. *Phys. Rev.*, D73:014020, 2006.
30. M. Anselmino, M. Boglione, U. D'Alesio, E. Leader, S. Melis, and F. Murgia. General helicity formalism for single and double spin asymmetries in $pp^\uparrow \rightarrow \pi X$. In *11th International Workshop on High Energy Spin Physics (DUBNA-SPIN-05) Dubna, Russia, September 27-October 1, 2005*.
31. M. Anselmino, M. Boglione, U. D'Alesio, E. Leader, and F. Murgia. Parton intrinsic motion: Suppression of the Collins mechanism for transverse single spin asymmetries in $pp^\uparrow \rightarrow \pi X$. *Phys. Rev.*, D71:014002, 2005.
32. M. Boglione, U. D'Alesio, and F. Murgia. Single spin asymmetries in inclusive hadron production from semi-inclusive DIS to hadronic collisions: Universality and phenomenology. *Phys. Rev.*, D77:051502, 2008.
33. Aram Kotzinian. New quark distributions and semiinclusive electroproduction on the polarized nucleons. *Nucl. Phys.*, B441:234–248, 1995.
34. R. D. Tangerman and P. J. Mulders. Intrinsic transverse momentum and the polarized Drell-Yan process. *Phys. Rev.*, D51:3357–3372, 1995.
35. R. D. Tangerman and P. J. Mulders. Probing transverse quark polarization in deep inelastic lepton production. *Phys. Lett.*, B352:129–133, 1995.
36. A. Airapetian et al. Single-spin asymmetries in semi-inclusive deep-inelastic scattering on a transversely polarized hydrogen target. *Phys. Rev. Lett.*, 94:012002, 2005.
37. V. Yu. Alexakhin et al. First measurement of the transverse spin asymmetries of the deuteron in semi-inclusive deep inelastic scattering. *Phys. Rev. Lett.*, 94:202002, 2005.
38. A. Airapetian et al. Transverse target single-spin asymmetry in inclusive electroproduction of charged pions and kaons. *Phys. Lett.*, B728:183–190, 2014.
39. C. Adolph et al. Measurement of azimuthal hadron asymmetries in semi-inclusive deep inelastic scattering off unpolarised nucleons. *Nucl. Phys.*, B886:1046–1077, 2014.
40. A. Airapetian et al. Multiplicities of charged pions and kaons from semi-inclusive deep-inelastic scattering by the proton and the deuteron. *Phys. Rev.*, D87:074029, 2013.
41. C. Adolph et al. Hadron Transverse Momentum Distributions in Muon Deep Inelastic Scattering at 160 GeV/c. *Eur. Phys. J.*, C73:2531, 2013.
42. Andrea Signori, Alessandro Bacchetta, Marco Radici, and Gunar Schnell. Investigations into the flavor dependence of partonic transverse momentum. *JHEP*, 1311:194, 2013.
43. M. Anselmino, M. Boglione, J.O. Gonzalez Hernandez, S. Melis, and A. Prokudin. Unpolarised Transverse Momentum Dependent Distribution and Fragmentation Functions from SIDIS Multiplicities. *JHEP*, 1404:005, 2014.
44. A. Airapetian et al. Azimuthal distributions of charged hadrons, pions, and kaons produced in deep-inelastic scattering off unpolarized protons and deuterons. *Phys. Rev.*, D87:012010, 2013.
45. V. Barone, M. Boglione, J.O. Gonzalez Hernandez, and S. Melis. Phenomenological analysis of azimuthal asymmetries in unpolarized semi-inclusive deep inelastic scattering. *Phys. Rev.*, D91(7):074019, 2015.
46. Bakur Parsamyan. Transverse spin azimuthal asymmetries in SIDIS at COMPASS: Multidimensional analysis. 2015.
47. K. Abe et al. Measurement of azimuthal asymmetries in inclusive production of hadron pairs in e^+e^- annihilation at Belle. *Phys. Rev. Lett.*, 96:232002, 2006.
48. M. Anselmino, M. Boglione, U. D'Alesio, A. Kotzinian, F. Murgia, et al. Transversity and Collins functions from SIDIS and e^+e^- data. *Phys. Rev.*, D75:054032, 2007.
49. M. Anselmino, M. Boglione, U. D'Alesio, A. Kotzinian, F. Murgia, et al. Update on transversity and Collins functions from SIDIS and e^+e^- data. *Nucl. Phys. Proc. Suppl.*, 191:98–107, 2009.
50. R. Seidl et al. Measurement of Azimuthal Asymmetries in Inclusive Production of Hadron Pairs in e^+e^- Annihilation at $\sqrt{s} = 10.58$ GeV. *Phys. Rev.*, D78:032011, 2008.
51. R. Seidl et al. Measurement of Azimuthal Asymmetries in Inclusive Production of Hadron Pairs in e^+e^- Annihilation at $\sqrt{s} = 10.58$ GeV. *Phys. Rev.*, D86:032011(E), 2012.
52. J.P. Lees et al. Measurement of Collins asymmetries in inclusive production of charged pion pairs in e^+e^- annihilation at BABAR. *Phys. Rev.*, D90(5):052003, 2014.
53. M. Anselmino, M. Boglione, U. D'Alesio, S. Melis, F. Murgia, et al. Simultaneous extraction of transversity and Collins functions from new SIDIS and e^+e^- data. *Phys. Rev.*, D87:094019, 2013.
54. Zhong-Bo Kang, Alexei Prokudin, Peng Sun, and Feng Yuan. Nucleon tensor charge from Collins azimuthal asymmetry measurements. *Phys. Rev.*, D91:071501, 2015.
55. Alessandro Bacchetta, Miguel G. Echevarria, Piet J. G. Mulders, Marco Radici, and Andrea Signori. Effects of TMD evolution and partonic flavor on e^+e^- annihilation into hadrons. 2015.
56. M. Anselmino, M. Boglione, U. D'Alesio, J. O. Gonzalez Hernandez, S. Melis, F. Murgia, and A. Prokudin. Collins functions for pions from SIDIS and new e^+e^- data: a first glance at their transverse momentum dependence. 2015.
57. Alessandro Bacchetta, Aurore Courtoy, and Marco Radici. First glances at the transversity parton distribution through dihadron fragmentation functions. *Phys. Rev. Lett.*, 107:012001, 2011.

58. Aurore Courtoy, Alessandro Bacchetta, Marco Radici, and Andrea Bianconi. First extraction of Interference Fragmentation Functions from e^+e^- data. *Phys. Rev.*, D85:114023, 2012.
59. Alessandro Bacchetta, A. Courtoy, and Marco Radici. First extraction of valence transversities in a collinear framework. *JHEP*, 1303:119, 2013.
60. S. Mert Aybat and Ted C. Rogers. TMD Parton Distribution and Fragmentation Functions with QCD Evolution. *Phys. Rev.*, D83:114042, 2011.
61. S. Mert Aybat, John C. Collins, Jian-Wei Qiu, and Ted C. Rogers. The QCD Evolution of the Sivers Function. *Phys. Rev.*, D85:034043, 2012.
62. S. Mert Aybat, Alexei Prokudin, and Ted C. Rogers. Calculation of TMD Evolution for Transverse Single Spin Asymmetry Measurements. *Phys. Rev. Lett.*, 108:242003, 2012.
63. M. Anselmino, M. Boglione, and S. Melis. A Strategy towards the extraction of the Sivers function with TMD evolution. *Phys. Rev.*, D86:014028, 2012.
64. M. Anselmino et al. The role of cahn and sivers effects in deep inelastic scattering. *Phys. Rev.*, D71:074006, 2005.
65. J. J. Aubert et al. Measurement of Hadronic Azimuthal Distributions in Deep Inelastic Muon Proton Scattering. *Phys. Lett.*, B130:118, 1983.
66. M. Arneodo et al. Measurement of Hadron Azimuthal Distributions in Deep Inelastic Muon Proton Scattering. *Z. Phys.*, C34:277, 1987.
67. P. Schweitzer, T. Teckentrup, and A. Metz. Intrinsic transverse parton momenta in deeply inelastic reactions. *Phys. Rev.*, D81:094019, 2010.
68. Bernhard U. Musch, Philipp Hagler, Andreas Schafer, Meinulf Gockeler, Dru Bryant Renner, and John W. Negele. Transverse momentum distributions of quarks from the lattice using extended gauge links. *PoS, LAT2007*:155, 2007.
69. Peng Sun, Joshua Isaacson, C. P. Yuan, and Feng Yuan. Universal Non-perturbative Functions for SIDIS and Drell-Yan Processes. 2014.
70. M. Boglione, J. O. Gonzalez Hernandez, S. Melis, and A. Prokudin. A study on the interplay between perturbative QCD and CSS/TMD formalism in SIDIS processes. *JHEP*, 02:095, 2015.
71. Alessandro Bacchetta and Marco Radici. Constraining quark angular momentum through semi-inclusive measurements. *Phys. Rev. Lett.*, 107:212001, 2011.
72. A. Accardi et al. Electron Ion Collider: The Next QCD Frontier - Understanding the glue that binds us all. 2012.
73. M. Anselmino, M. Boglione, U. D'Alesio, S. Melis, F. Murgia, and A. Prokudin. New insight on the Sivers transverse momentum dependent distribution function. *J. Phys. Conf. Ser.*, 295:012062, 2011.
74. M. Anselmino, M. Boglione, U. D'Alesio, A. Kotzinian, F. Murgia, and A. Prokudin. Extracting the Sivers function from polarized SIDIS data and making predictions. *Phys. Rev.*, D72:094007, 2005. [Erratum: *Phys. Rev.* D72:099903(2005)].
75. M. Anselmino et al. Comparing extractions of Sivers functions. *Transversity. Proceedings, Workshop, Como, Italy, September 7-10, 2005*, pages 236–243, 2005.
76. J. C. Collins, A. V. Efremov, K. Goeke, S. Menzel, A. Metz, and P. Schweitzer. Sivers effect in semi-inclusive deeply inelastic scattering. *Phys. Rev.*, D73:014021, 2006.
77. Werner Vogelsang and Feng Yuan. Single-transverse spin asymmetries: From DIS to hadronic collisions. *Phys. Rev.*, D72:054028, 2005.
78. M. Anselmino, M. Boglione, U. D'Alesio, A. Kotzinian, S. Melis, F. Murgia, A. Prokudin, and C. Turk. Sivers Effect for Pion and Kaon Production in Semi-Inclusive Deep Inelastic Scattering. *Eur. Phys. J.*, A39:89–100, 2009.
79. Miguel G. Echevarria, Ahmad Idilbi, and Ignazio Scimemi. Soft and Collinear Factorization and Transverse Momentum Dependent Parton Distribution Functions. *Phys. Lett.*, B726:795–801, 2013.
80. Miguel G. Echevarria, Ahmad Idilbi, Andreas Schfer, and Ignazio Scimemi. Model-Independent Evolution of Transverse Momentum Dependent Distribution Functions (TMDs) at NNLL. *Eur. Phys. J.*, C73(12):2636, 2013.
81. M. Anselmino, M. Boglione, U. D'Alesio, S. Melis, F. Murgia, and A. Prokudin. Sivers Distribution Functions and the Latest SIDIS Data. In *19th International Workshop on Deep-Inelastic Scattering and Related Subjects (DIS 2011) Newport News, Virginia, April 11-15, 2011*, 2011.
82. A. Airapetian et al. Observation of the Naive-T-odd Sivers Effect in Deep-Inelastic Scattering. *Phys. Rev. Lett.*, 103:152002, 2009.
83. F. Bradamante. New COMPASS results on Collins and Sivers asymmetries. *Nuovo Cim.*, C035N2:107–114, 2012.
84. M. Anselmino, M. Boglione, U. D'Alesio, S. Melis, F. Murgia, E. R. Nocera, and A. Prokudin. General Helicity Formalism for Polarized Semi-Inclusive Deep Inelastic Scattering. *Phys. Rev.*, D83:114019, 2011.
85. Peng Sun and Feng Yuan. Energy Evolution for the Sivers Asymmetries in Hard Processes. *Phys. Rev.*, D88:034016, 2013.
86. Xiang-dong Ji, Jian-ping Ma, and Feng Yuan. QCD factorization for semi-inclusive deep-inelastic scattering at low transverse momentum. *Phys. Rev.*, D71:034005, 2005.
87. Miguel G. Echevarria, Ahmad Idilbi, Zhong-Bo Kang, and Ivan Vitev. QCD Evolution of the Sivers Asymmetry. *Phys. Rev.*, D89:074013, 2014.
88. Daniel Boer, P. J. Mulders, and F. Pijlman. Universality of T odd effects in single spin and azimuthal asymmetries. *Nucl. Phys.*, B667:201–241, 2003.
89. Zhong-Bo Kang, Jian-Wei Qiu, Werner Vogelsang, and Feng Yuan. An Observation Concerning the Process Dependence of the Sivers Functions. *Phys. Rev.*, D83:094001, 2011.
90. Koichi Kanazawa, Yuji Koike, Andreas Metz, and Daniel Pitonyak. Towards an explanation of transverse single-spin asymmetries in proton-proton collisions: the role of fragmentation in collinear factorization. *Phys. Rev.*, D89(11):111501, 2014.
91. A. V. Efremov, K. Goeke, S. Menzel, A. Metz, and P. Schweitzer. Sivers effect in semi-inclusive DIS and in the Drell-Yan process. *Phys. Lett.*, B612:233–244, 2005.
92. M. Anselmino, M. Boglione, U. D'Alesio, S. Melis, F. Murgia, and A. Prokudin. Sivers effect in Drell-Yan processes. *Phys. Rev.*, D79:054010, 2009.
93. M. Boglione and S. Melis. Polarized and unpolarized Drell-Yan angular distribution in the helicity formalism. *Phys. Rev.*, D84:034038, 2011.

94. Zhong-Bo Kang and Jian-Wei Qiu. Testing the Time-Reversal Modified Universality of the Siverson Function. *Phys. Rev. Lett.*, 103:172001, 2009.
95. Rohini M. Godbole, Abhiram Kaushik, Anuradha Misra, and Vaibhav S. Rawoot. Single Spin Asymmetry in Electroproduction of J/ψ and QCD-evolved TMD's. *Int. J. Mod. Phys. Conf. Ser.*, 37:1560069, 2015.
96. A. Metz. Gluon-exchange in spin-dependent fragmentation. *Phys. Lett.*, B549:139–145, 2002.
97. John C. Collins and Andreas Metz. Universality of soft and collinear factors in hard-scattering factorization. *Phys. Rev. Lett.*, 93:252001, 2004.
98. M. Ablikim et al. Measurement of azimuthal asymmetries in inclusive charged dipion production in e^+e^- annihilations at $\sqrt{s} = 3.65$ GeV. 2015.
99. Alessandro Bacchetta, Umberto D'Alesio, Markus Diehl, and C. Andy Miller. Single-spin asymmetries: The Trento conventions. *Phys. Rev.*, D70:117504, 2004.
100. Daniel Boer. Angular dependences in inclusive two-hadron production at BELLE. *Nucl. Phys.*, B806:23–67, 2009.
101. D. Pitonyak, M. Schlegel, and A. Metz. Polarized hadron pair production from electron-positron annihilation. *Phys. Rev.*, D89(5):054032, 2014.
102. Gavin P. Salam and Juan Rojo. A Higher Order Perturbative Parton Evolution Toolkit (HOPPET). *Comput. Phys. Commun.*, 180:120–156, 2009.
103. Zhong-Bo Kang, Alexei Prokudin, Peng Sun, and Feng Yuan. Extraction of Quark Transversity Distribution and Collins Fragmentation Functions with QCD Evolution. 2015.
104. Feng Yuan and Jian Zhou. Collins Fragmentation and the Single Transverse Spin Asymmetry. *Phys. Rev. Lett.*, 103:052001, 2009.
105. Zhong-Bo Kang. QCD evolution of naive-time-reversal-odd fragmentation functions. *Phys. Rev.*, D83:036006, 2011.
106. Zhong-Bo Kang, Bo-Wen Xiao, and Feng Yuan. QCD Resummation for Single Spin Asymmetries. *Phys. Rev. Lett.*, 107:152002, 2011.
107. Alessandro Bacchetta and Alexei Prokudin. Evolution of the helicity and transversity Transverse-Momentum-Dependent parton distributions. *Nucl. Phys.*, B875:536–551, 2013.
108. Peng Sun and Feng Yuan. Transverse momentum dependent evolution: Matching semi-inclusive deep inelastic scattering processes to Drell-Yan and W/Z boson production. *Phys. Rev.*, D88(11):114012, 2013.
109. Miguel G. Echevarria, Ahmad Idilbi, and Ignazio Scimemi. Unified treatment of the QCD evolution of all (un-)polarized transverse momentum dependent functions: Collins function as a study case. *Phys. Rev.*, D90(1):014003, 2014.
110. Daniel Boer. Sudakov suppression in azimuthal spin asymmetries. *Nucl. Phys.*, B603:195–217, 2001.
111. Yuji Koike, Junji Nagashima, and Werner Vogelsang. Resummation for polarized semi-inclusive deep-inelastic scattering at small transverse momentum. *Nucl. Phys.*, B744:59–79, 2006.
112. Pavel M. Nadolsky, D. R. Stump, and C. P. Yuan. Semi-inclusive hadron production at HERA: The Effect of QCD gluon resummation. *Phys. Rev.*, D61:014003, 2000. [Erratum: *Phys. Rev.* D64,059903(2001)].
113. Daniel Boer and P. J. Mulders. Time reversal odd distribution functions in lepton production. *Phys. Rev.*, D57:5780–5786, 1998.
114. W. Kafer. Measurements of Unpolarized Azimuthal Asymmetries at COMPASS. 2008.
115. Andrea Bressan. Azimuthal asymmetries in SIDIS off unpolarized targets at COMPASS. 2009.
116. Francesca Giordano and Rebecca Lamb. Measurement of azimuthal asymmetries of the unpolarized cross section at HERMES. *AIP Conf. Proc.*, 1149:423–426, 2009.
117. Vincenzo Barone, Stefano Melis, and Alexei Prokudin. The Boer-Mulders effect in unpolarized SIDIS: An Analysis of the COMPASS and HERMES data on the $\cos 2\phi$ asymmetry. *Phys. Rev.*, D81:114026, 2010.
118. Vincenzo Barone, Alexei Prokudin, and Bo-Qiang Ma. A Systematic phenomenological study of the $\cos 2\phi$ asymmetry in unpolarized semi-inclusive DIS. *Phys. Rev.*, D78:045022, 2008.
119. Matthias Burkardt. Transverse deformation of parton distributions and transversity decomposition of angular momentum. *Phys. Rev.*, D72:094020, 2005.
120. M. Gockeler, Ph. Hagler, R. Horsley, Y. Nakamura, D. Pleiter, Paul E. L. Rakow, A. Schafer, G. Schierholz, H. Stuben, and J. M. Zanotti. Transverse spin structure of the nucleon from lattice QCD simulations. *Phys. Rev. Lett.*, 98:222001, 2007.
121. P. V. Pobylitsa. Transverse momentum dependent parton distributions in large N(c) QCD. 2003.
122. Leonard P. Gamberg, Gary R. Goldstein, and Marc Schlegel. Transverse Quark Spin Effects and the Flavor Dependence of the Boer-Mulders Function. *Phys. Rev.*, D77:094016, 2008.
123. Alessandro Bacchetta, Francesco Conti, and Marco Radici. Transverse-momentum distributions in a diquark spectator model. *Phys. Rev.*, D78:074010, 2008.
124. Barbara Pasquini and Feng Yuan. Siverson and Boer-Mulders functions in Light-Cone Quark Models. *Phys. Rev.*, D81:114013, 2010.
125. Vincenzo Barone, Stefano Melis, and Alexei Prokudin. Azimuthal asymmetries in unpolarized Drell-Yan processes and the Boer-Mulders distributions of antiquarks. *Phys. Rev.*, D82:114025, 2010.
126. M. Boglione, S. Melis, and A. Prokudin. Partonic Transverse Motion in Unpolarized Semi-Inclusive Deep Inelastic Scattering Processes. *Phys. Rev.*, D84:034033, 2011.
127. L. Y. Zhu et al. Measurement of Angular Distributions of Drell-Yan Dimuons in $p + d$ Interaction at 800-GeV/c. *Phys. Rev. Lett.*, 99:082301, 2007.
128. L. Y. Zhu et al. Measurement of Angular Distributions of Drell-Yan Dimuons in $p + p$ Interactions at 800-GeV/c. *Phys. Rev. Lett.*, 102:182001, 2009.
129. Christopher Lefky and Alexei Prokudin. Extraction of the distribution function h_{1T}^\perp from experimental data. *Phys. Rev.*, D91(3):034010, 2015.
130. P. J. Mulders and R. D. Tangerman. The Complete tree level result up to order $1/Q$ for polarized deep inelastic lepton production. *Nucl. Phys.*, B461:197–237, 1996. [Erratum: *Nucl. Phys.* B484,538(1997)].
131. Alessandro Bacchetta, Markus Diehl, Klaus Goeke, Andreas Metz, Piet J. Mulders, et al. Semi-inclusive deep inelastic scattering at small transverse momentum. *JHEP*, 0702:093, 2007.